ACS OMEGA

http://pubs.acs.org/journal/acsodf

Article

Mimicking the Cu Active Site of Lytic Polysaccharide Monooxygenase Using Monoanionic Tridentate N-Donor Ligands

Caitlin J. Bouchey, Dimitar Y. Shopov, Aaron D. Gruen, and William B. Tolman*

Cite This: *ACS Omega* 2022, 7, 35217−35232

Read Online

ACCESS | Metrics & More | Article Recommendations | Supporting Information

ABSTRACT: In an effort to prepare small molecule mimics of the active site of lytic polysaccharide monooxygenase (LPMO), three monoanionic tridentate N donor ligands comprising a central deprotonated amide group flanked by two neutral donors were prepared, and their coordination chemistry with Cu(I) and Cu(II) was evaluated. With Cu(I), a dimer formed, which was characterized by X-ray crystallography and NMR spectroscopy. A variety of mononuclear and dinuclear Cu(II) species with a range of auxiliary ligands (MeCN, Cl^-, OH^-, OAc^-, OBz^-, CO_3^{2-}) were prepared and characterized by X-ray diffraction and various spectroscopies (UV−vis, EPR). The complexes exhibit structural similarities to the LPMO active site.

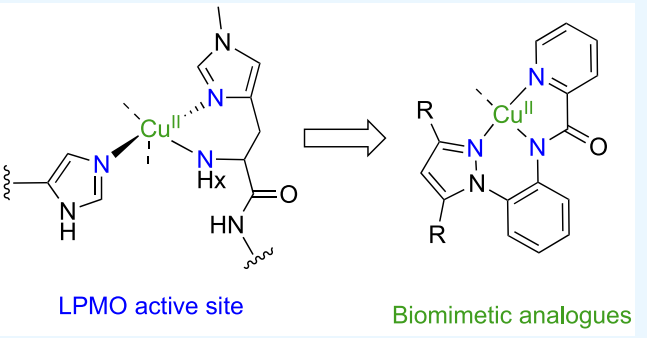

INTRODUCTION

In the subject area of challenging substrate oxidations by copper enzymes,[1] lytic polysaccharide monooxygenase (LPMO) is an important biological example of a catalyst capable of activating dioxygen to cleave strong C−H bonds, which in this case are those in cellulose and associated polymers, to yield short-chain oligomers.[2−6] While the structure of LPMO and its active site are well-known,[7,8] the precise mechanism of oxygen activation and subsequent oxidation of the cellulose substrate and how the structural motif of the active site of LPMO supports these processes remains the subject of extensive research efforts.

The active site of LPMO contains a mononuclear copper center with three conserved coordinating groups: two histidine residues and a more unusual third group, the amine terminus of the protein chain (Figure 1). This terminus belongs to one of the coordinating histidine residues, thereby forming a metalacyclic moiety dubbed the "histidine brace".[8] The enzyme is unreactive when the Cu center is in the +2 oxidation state, but upon reduction to Cu(I) the active site can react with O_2 to generate an oxidizing species.[9] The protonation state of the ligands is ambiguous, with neutral or monoanionic environments having been proposed.[10−12] Even though the specific Cu species responsible for the proposed rate-determining step of hydrogen atom transfer (HAT) from saccharide substrates is unknown, several Cu−oxygen cores have been implicated, such as $[Cu{-}OO]^+$, $[Cu{-}OH]^{2+}$, and $[Cu{-}O]^+$.[8,10,13−20] These cores have been studied in model complexes, in the gas phase, and/or computationally and have been shown to be competent at HAT from various O−H and C−H bonds.

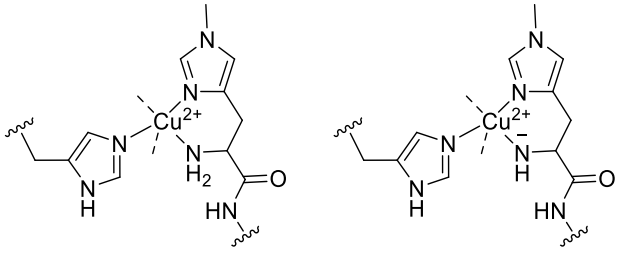

Figure 1. Proposed active site of lytic polysaccharide monooxygenase (LPMO) enzymes: neutral (left) and monoanionic (right) states showing only the conserved supporting ligands.

In previous work, formally Cu(III) species with $[Cu{-}OH]^{2+}$ cores using a family of dianionic pyridine dicarboxamide supporting ligands (Figure 2) were prepared and shown to perform proton-coupled electron transfer (PCET) reactions rapidly.[22−28] The two strongly electron-donating carboxamide donors of these ligands stabilize such oxidized species, but on the other hand, they hinder formation of Cu(I) complexes. As a result, it is not possible to use biomimetic $Cu(I)/O_2$ reactions[32] directly with these ligands to produce reactive cores such as $[Cu{-}OO]^+$. Instead, this core was accessed by introduction of free superoxide to Cu(II) precursors.[29−31,33,34]

Received: July 13, 2022
Accepted: September 2, 2022
Published: September 23, 2022

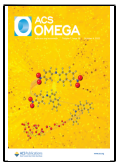

https://doi.org/10.1021/acsomega.2c04432
ACS Omega 2022, 7, 35217−35232

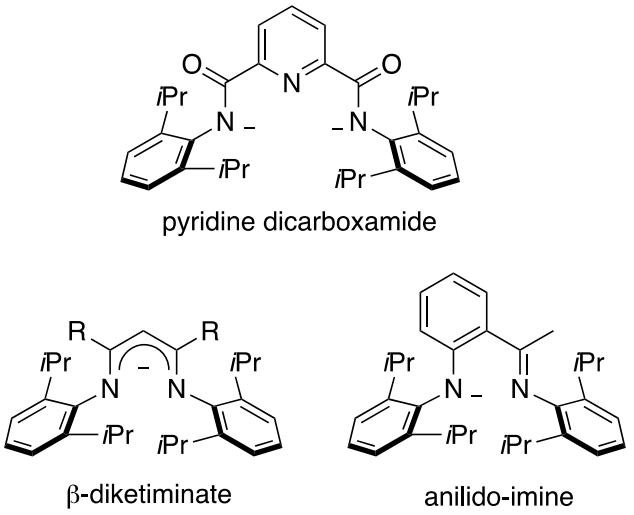

Figure 2. Previously studied ligands used to study Cu−oxygen chemistry.

With the goal of examining the effects of changing the supporting ligand charge, we sought to design pincer ligands that placed a carboxamido group in the central position with flanking neutral N donors. We hypothesized this monoanionic donor set would mimic the postulated deprotonated histidine brace of LPMO and sufficiently decrease the overall donor strength, allowing us to access the Cu(I) state and enabling reactions with O_2 to be observed, while potentially retaining the accessibility of the formally Cu(III) state. In support of this hypothesis, many mononuclear Cu−O_2 adducts that are formed by the reaction of Cu(I) complexes with dioxygen feature monoanionic supporting ligands, although these are typically bidentate, such as β-diketiminates or anilido-imines (Figure 2).[21,35,36] These adducts typically exist as transient and/or side-on species.[21,37,38] We speculated that adding a third arm to a similar ligand motif could force the formation of end-on copper−dioxygen species akin to that proposed for LPMO[9] by blocking the extra coordination site of the Cu center.

Thus inspired, we designed three new ligands that provide a N-donor ligand environment analogous to the proposed deprotonated active site of LPMO, employing an anionic amido group within a tridentate framework. These ligands, derived from the proligands **HL^1**−**HL^3** (Figure 3), feature a pyridine carboxamido fragment paired with either a pyrazolyl (**HL^1** or **HL^2**) or trisubstituted imine group (**HL^3**). This design places the carboxamido unit in the middle position, similar to what is present in LPMO, from where it could, in principle, influence charge delocalization and reactivity of the bound dioxygen moiety. Herein, we report success in synthesizing the target ligands and exploring their copper coordination chemistry. Ultimately, however, our efforts to generate reactive copper−oxygen species were thwarted. Nonetheless, the fundamental advances in coordination chemistry we describe through the development of new ligands and complexes provides a foundation for future work, as literature examples of Cu complexes with monoanionic N,N′,N′′ ligands employing a central anionic group are fairly limited.[39−69] We are hopeful that further modifications of the scaffolds we have studied here could yield future successes with copper−oxygen chemistry.

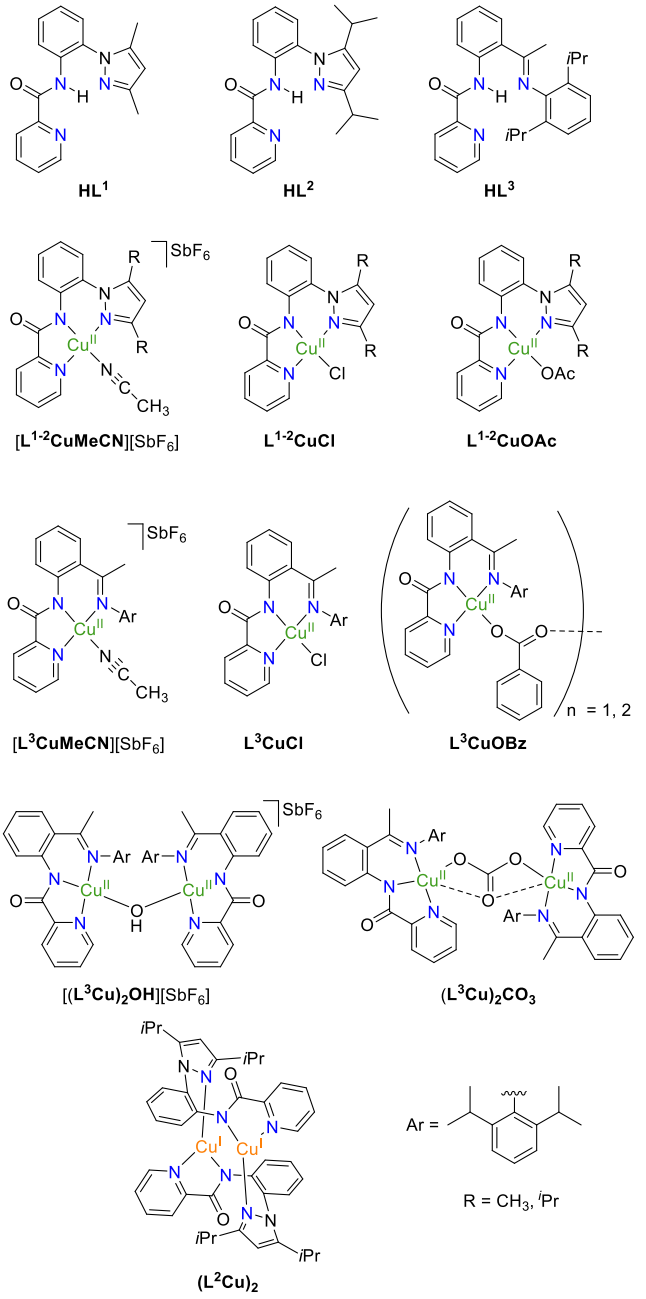

Figure 3. Proligands and derived complexes prepared in this work.

RESULTS AND DISCUSSION

Ligand Synthesis. The pyridine−carboxamide−pyrazole proligands **HL^1** and **HL^2** were synthesized in three steps, in a similar fashion to a previous report,[70] where a nucleophilic aromatic substitution of 1-fluoro-2-nitrobenzene with NaH and 3,5-subsituted pyrazoles yielded the pyrazole-substituted nitrobenzene compounds, which were reduced to anilines via palladium-catalyzed hydrogenation (Scheme 1). These anilines were converted to the final proligands in overall yields of 59% and 44% for **HL^1** and **HL^2**, respectively, via reaction with picolinoyl acid chloride, prepared in situ from oxalyl chloride and picolinic acid. The pyridine−carboxamide−imine proligand **HL^3** was synthesized in two steps by performing an amidation reaction between 2-aminoacetophenone and picolinic acid using tosyl chloride and triethylamine, as

https://doi.org/10.1021/acsomega.2c04432
ACS Omega 2022, 7, 35217−35232

Scheme 1. Syntheses of the Proligands HL^{1-3} Used in This Work

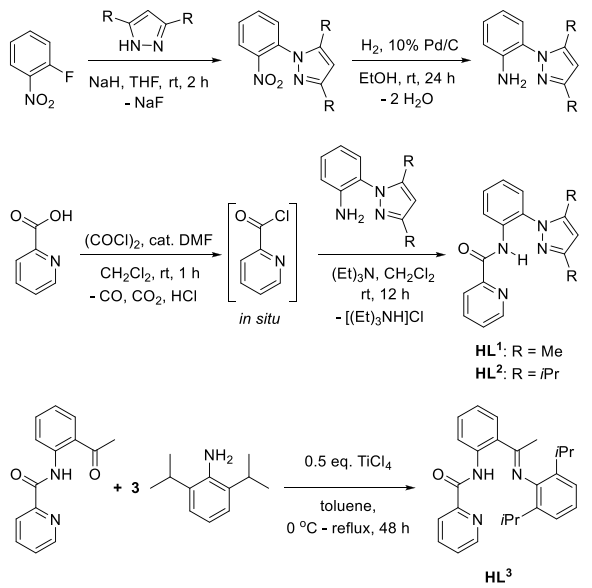

previously reported,[71] then assembling the final proligand via a $TiCl_4$-aided condensation between the newly formed ketone and 2,6-diisopropylaniline in an overall yield of 25−33%. The low yield is mostly due to the latter step, as the imine condensation between these two reactants proved to be problematic, being inaccessible by several other routes and only poorly afforded by the one we utilized. Nonetheless, gram amounts of ligand could be prepared due to the readily available starting materials. The formulations of the intermediates and the three proligands were established by ^1H and $^{13}C\{^1H\}$ NMR spectroscopy (Figures S1−S13) and elemental analysis.

Cu(I) Metalation. Since the active site of LPMO uses a Cu(I) center to reduce oxygen, we sought to synthesize a mononuclear Cu(I) complex by reacting HL^2 with K[N-$(SiMe_3)_2$] (KHMDS) and $Cu(MeCN)_4OTf$ in MeCN (Scheme 2). The resulting orange compound was characterized by NMR spectroscopy, UV−visible spectroscopy, cyclic voltammetry, CHN analysis, and X-ray diffraction. The ^1H NMR spectrum (Figure S14) of the new species depicted a loss of the amide N−H resonance and an upfield shift of all resonances relative to the spectrum of HL^2. In addition, separate peaks for the methyl groups on the iPr substituents were observed in both the ^1H NMR and $^{13}C\{^1H\}$ NMR spectra, the latter of which contain the full complement of 21 peaks (Figure S14). These data indicate deprotonation of HL^2 and coordination to a copper ion(s). Such coordination is also supported by the presence of absorption features in the UV−vis spectrum of the orange product (Figure S15) at 426 nm (ε = 16490 M^{-1} cm^{-1}) and 592 nm (ε = 1365 M^{-1} cm^{-1}).

Scheme 2. Metalation of HL^2 with Cu(I)

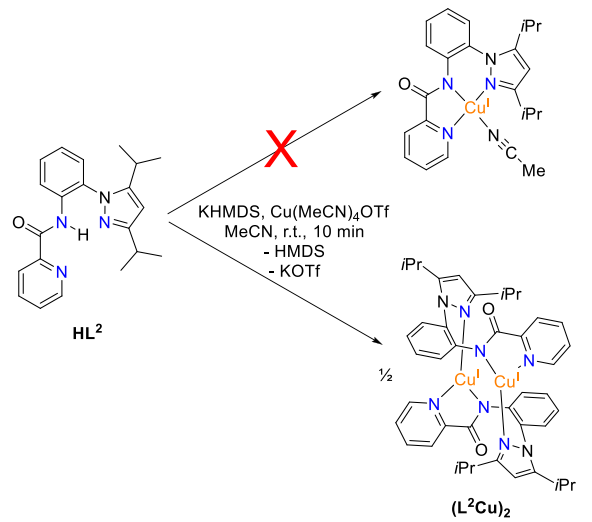

The X-ray crystal structure (Figure 4) revealed that instead of being mononuclear the compound is a dimer, $(L^2Cu)_2$,

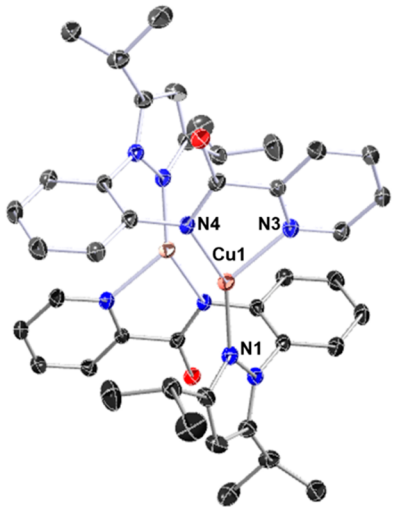

Figure 4. X-ray crystal structure of $(L^2Cu)_2$ with the THF molecules and H atoms omitted for clarity. Atoms are shown as 30% thermal ellipsoids. Selected bond distances (Å) and angles (deg): Cu1−N1, 1.909(2); Cu1−N3, 1.935(2); Cu1−N4, 2.151(2); N1−Cu1−N3, 155.79(9); N1−Cu1−N4, 118.13(9); N3−Cu1−N4, 81.90(9).

where each ligand bridges the two copper ions in a (κ^1, κ^2) fashion. The Cu(I) ions adopt distorted trigonal planar geometries. The Cu−N lengths are typical for similar Cu(I) complexes,[44,45,49,60] and the Cu−Cu distance is 2.7509(7) Å, which is too long for significant bonding interactions between the two metals.[72]

Although the solid-state structure shows the formation of a dimer for the 1:1 Cu(I)/L^2 complex, it is not clear if the dimeric structure is retained in solution. Some species, like tris(pyrazolyl)hydroborate Cu(I) complexes, have been shown to crystallize as dimers, but the solution-state data suggests the dimers can dissociate in solution to monomeric units.[73,74] The solution NMR data are consistent with both the hypothesized monomer in Scheme 1 and $(L^2Cu)_2$, as the symmetry of the solid-state dimer structure would result in only one set of ligand resonances.

Even not knowing the nuclearity in solution, and because Cu(I) dimers can activate small molecules,[75,76] we examined the reactivity of the Cu(I) complex in solution with O_2 in an attempt to access and stabilize a 1:1:1 L^2/Cu/O_2 adduct. Thus, we bubbled gaseous O_2 into a THF solution of $(L^2Cu)_2$ at −80 °C for 2 min. There were no apparent changes in the spectrum, indicating no reaction with O_2 at this temperature (Figure S15). Additionally, no spectral changes were observed upon

https://doi.org/10.1021/acsomega.2c04432
ACS Omega 2022, 7, 35217−35232

warming the solution in the presence of O_2. This unfortunate lack of reactivity of the Cu(I) complex contrasts with the reactivity of other species supported by tridentate monoanionic N-donor ligands,[77,78] the reasons for which are unknown.

Cyclic voltammetry experiments using THF solutions of $(\mathbf{L^2Cu})_2$ revealed an irreversible oxidation event at 170 mV vs Fc/Fc^+ (Figure S24; scan rate 100 mV s^{-1}; 0.3 M Bu_4NPF_6). When cycling past this oxidation event, another irreversible reduction occurs on the reducing sweep at −83 mV vs Fc/Fc^+. However, this reduction event is not observed when performing the reductive sweep without first undergoing oxidation. This finding is suggestive of a highly hysteretic Cu(I/II) redox process whereby oxidation generates a Cu(II) complex that undergoes a chemical transformation to a species that is then reduced at the low potential. We speculate that this species may be a monomeric Cu(II) compound on the basis of observed formation of such complexes in other synthetic reactions described below.

Cu(II)-Cl Complexes Bearing $(L^1)^-$ and $(L^2)^-$. We reacted $\mathbf{HL^1}$ and $\mathbf{HL^2}$ with multiple Cu(II) sources with the aim of preparing mononuclear copper complexes. Deprotonation of $\mathbf{HL^1}$ and $\mathbf{HL^2}$ with KHMDS followed by reaction with anhydrous $CuCl_2$ yielded dark green products that were characterized by UV−vis and EPR spectroscopy, elemental analysis, and X-ray crystallography. Crystalline samples that were suitable for X-ray diffraction were obtained and revealed the products to be $\mathbf{L^1CuCl}$ and $\mathbf{L^2CuCl}$ (Figure 5). In the solid state, $\mathbf{L^2CuCl}$ exists as a dimer composed of two $\mathbf{L^2CuCl}$ units where the Cl from one unit has a weak interaction in the axial position of the Cu in the other unit (2.7025(9) and 2.7464(9) Å), a motif seen in other Cu(II)−halide complexes supported by tridentate ligands.[67,68,79−84] On the other hand, $\mathbf{L^1CuCl}$ does not exhibit the same phenomenon, remaining monomeric in the solid state, as seen in other similar Cu(II)−halide complexes.[40,41,43,85,86] The bond lengths are comparable between the two complexes, but all of the bond lengths were slightly shorter in $\mathbf{L^1CuCl}$, and the geometry index values, τ_4, of the metal centers are 0.37 and 0.31 for $\mathbf{L^1CuCl}$ and $\mathbf{L^2CuCl}$, respectively, indicating moderate deviation from a square planar geometry. Compared to a known Cu(II)−Cl structure of LPMO,[7] the Cu−N and Cu−Cl distances are similar (Cu−N(his): 2.0 Å on average in the LPMO structure and Cu−N(pyridine, pyrazole): 1.99 and 2.03 Å on average in $\mathbf{L^1CuCl}$ and $\mathbf{L^2CuCl}$, respectively; Cu−$N(NH_2)$: 2.2 Å in the LPMO structure and Cu−N(NH): 1.93 and 1.95 in $\mathbf{L^1CuCl}$ and $\mathbf{L^2CuCl}$, respectively; Cu−Cl 2.3 Å in the LPMO structure and 2.21 and 2.27 Å in $\mathbf{L^1CuCl}$ and $\mathbf{L^2CuCl}$, respectively). However, the geometries about the Cu ions in $\mathbf{L^1CuCl}$ and $\mathbf{L^2CuCl}$ deviate from square planar geometries more than in the LPMO structure (τ_4 of 0.11).[7]

The complexes $\mathbf{L^1CuCl}$ and $\mathbf{L^2CuCl}$ were also characterized by EPR spectroscopy (THF, X-band, 30 K, Figure S36) which showed signals typical for tetragonal, monomeric Cu(II) complexes, indicating that the dimeric solid-state structure for the latter complex does not persist in solution. The simulated g values (Table S1) support some degree of rhombicity. Both EPR spectra show Cu hyperfine and N superhyperfine splitting, the parameters for which were determined by simulation (Table S1). The UV−vis spectra of the complexes (in MeCN) have weak features consistent with d−d transitions in Cu(II) species (Figure S16; $\mathbf{L^1CuCl}$: 463 nm (ε = 358 M^{-1} cm^{-1}), 604 nm (ε = 152 M^{-1} cm^{-1}), 775 nm (ε = 198 M^{-1} cm^{-1}); $\mathbf{L^2CuCl}$: 458 nm (ε = 325 M^{-1} cm^{-1}), 606 nm (ε = 105 M^{-1} cm^{-1}), and 815 nm (ε = 177 M^{-1} cm^{-1})). Taken together, the data show that mononuclear Cu(II) complexes containing $(\mathbf{L^1})^-$ and $(\mathbf{L^2})^-$ can be synthesized, and they model the histidine brace of LPMO.

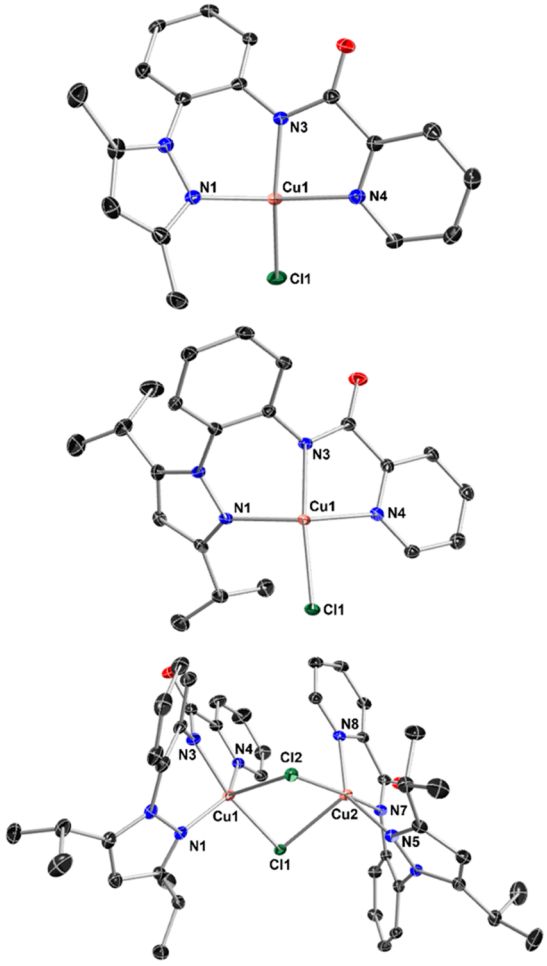

Figure 5. X-ray crystal structures of $\mathbf{L^1CuCl}$ (top) and $\mathbf{L^2CuCl}$ (middle) and a representation of the solid-state electrostatic dimer of $\mathbf{L^2CuCl}$ (bottom). H atoms are omitted for clarity, and all non-H atoms are shown as 30% thermal ellipsoids. Selected bond distances (Å) and angles (deg) for $\mathbf{L^1CuCl}$: Cu1−N1, 1.9909(16); Cu1−N3, 1.9341(15); Cu1−N4, 1.9999(17); Cu1−Cl1, 2.2059(5); N1−Cu1−N4, 149.41(7); N3−Cu1−Cl1, 158.01(5). Selected bond distances (Å) and angles (deg) for $\mathbf{L^2CuCl}$: Cu1−N1, 2.032(3); Cu1−N3, 1.947(3); Cu1−N4, 2.030(3); Cu1−Cl1, 2.2701(9); Cu1−Cl2, 2.7025(9); N1−Cu1−N4, 144.64(12); N3−Cu1−Cl1, 171.00(9).

Cu(II)−Solvento Complexes Bearing $(L^1)^-$ and $(L^2)^-$. While the chloro complexes are stable and useful for structural assessment, we sought compounds that could more readily be converted to various copper−oxygen species by virtue of the presence of a labile ligand such as MeCN. To this end, we deprotonated $\mathbf{HL^1}$ and $\mathbf{HL^2}$ with KHMDS in MeCN and then added $[Cu(MeCN)_5][SbF_6]_2$ to the solutions. The resulting green products were characterized by EPR and UV−vis spectroscopy, elemental analysis, and high-resolution electrospray ionization−mass spectrometry (HR ESI-MS, Figure S34). On the basis of these data we tentatively propose the formulations $[\mathbf{L^1CuMeCN}][SbF_6]$ and $[\mathbf{L^2CuMeCN}][SbF_6]$. Thus, the EPR spectra (Figure S37) reveal the unpaired spins are localized on the Cu(II) ions, as evidenced by the hyperfine

https://doi.org/10.1021/acsomega.2c04432
ACS Omega 2022, 7, 35217−35232

interactions in the $g_{parallel}$ region of the pseudoaxial signal, but superhyperfine splitting from the N atoms is not apparent (parameters listed in Table S2). The UV−vis spectra of the complexes in MeCN were measured, with that of [$\mathbf{L^1CuMeCN}$][SbF_6] having features at 466 nm (ε = 390 M^{-1} cm^{-1}) and 731 nm (ε = 220 M^{-1} cm^{-1}) and that of [$\mathbf{L^2CuMeCN}$][SbF_6] having similar absorptions at 462 nm (ε = 255 M^{-1} cm^{-1}) and 752 nm (ε = 122 M^{-1} cm^{-1}) (Figure S18). These low absorbing peaks are consistent with *d*−*d* transitions typical in Cu(II) complexes, but they are different from the features found for $\mathbf{L^1CuCl}$ and $\mathbf{L^2CuCl}$, consistent with a different fourth ligand that perturbs the electronic structure of the complex. Unfortunately, attempted elemental analyses were inconclusive, as the results were inconsistent with the proposed structures and could not be fit to a combination of metals, ligands, solvents, and contaminants, possibly due to a variety of ligands being present in the fourth coordination site of the copper (i.e., other solvents or a carbonyl from a neighboring molecule), or additional solvent coordination on the fifth position. In view of this issue, high-resolution ESI-MS data were collected for acetonitrile solutions of the complexes and yielded positive ion peak envelopes that may be assigned to 1:1 $\mathbf{L^n}$/Cu (**n** = 1 and 2) species with no bound acetonitrile (Figure S34). Attempts to obtain X-ray crystal structures of [$\mathbf{L^1CuMeCN}$][SbF_6] and [$\mathbf{L^2CuMeCN}$][SbF_6] were unsuccessful, despite exhaustive efforts to grow crystals suitable for X-ray diffraction and microcrystal electron diffraction. Ultimately, the nature of the species formed in solution remained uncertain, so alternative syntheses to discrete Cu(II) species were explored.

Cu(II)-OAc Complexes Bearing $(L^1)^-$ and $(L^2)^-$. In a different synthetic route, we reacted $\mathbf{HL^1}$ and $\mathbf{HL^2}$ with $Cu(OAc)_2{\cdot}H_2O$ in the presence of 3 Å molecular sieves in MeCN, which yielded vibrant green-blue products. Both products were characterized by X-ray crystallography, EPR and UV−vis spectroscopy, and elemental analysis. X-ray diffraction quality crystals of both products were obtained, and the structures revealed the products to be $\mathbf{L^1CuOAc}$ and $\mathbf{L^2CuOAc}$ (Figure 6). The acetate ligands are bound in monodentate fashion with weak interactions from the second carboxylate oxygens in the axial position of the Cu(II) ion (Cu−O3 lengths: 2.611(5) Å for $\mathbf{L^1CuOAc}$ and 2.3310(19) Å for $\mathbf{L^2CuOAc}$). The geometric parameter, τ_4, of the metal center is about equal for each complex: 0.33 for $\mathbf{L^1CuOAc}$ and 0.36 for $\mathbf{L^2CuOAc}$. All other bond lengths in the two compounds are similar. The solid-state structures resemble those of other Cu(II)-acetate complexes supported by tridentate ligands.[43,46,54,57,59,63,66,69,87,88] The Cu−N distances found for $\mathbf{L^1CuOAc}$ and $\mathbf{L^2CuOAc}$ are all similar to previously published structures, and the Cu−O2 bond lengths of 1.920 and 1.9492 Å are within the range of the known Cu−O(proximal)OCH_3 bond lengths (1.92−2.08 Å). The Cu−O(distal)OCH_3 lengths of 2.611(5) and 2.3310(19) Å are also within or very similar to the range found for the previously reported similar Cu(II)−acetate structures (2.37−2.85 Å). Previously, LPMO and fungal LPMO-like copper proteins were discovered to contain a Cu(II) ligated by the histidine brace and a carboxylate residue. The binding of the carboxylate ligands to copper in $\mathbf{L^1CuOAc}$ and $\mathbf{L^2CuOAc}$ bear a resemblance to those in the protein structures, where a Cu−O bond (1.98−2.16 Å) is in the histidine brace plane and a Cu−O interaction (2.68−3.07 Å) is in an axial position of the copper.[89−91]

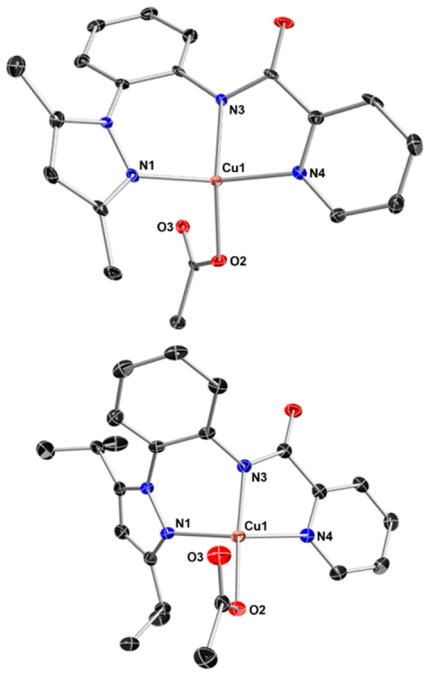

Figure 6. X-ray crystal structures of $\mathbf{L^1CuOAc}$ (left) and $\mathbf{L^2CuOAc}$ (right). H atoms are omitted for clarity, and all non-H atoms are shown as 30% thermal ellipsoids. Selected bond distances (Å) and angles (deg) for $\mathbf{L^1CuOAc}$: Cu1−N1, 2.018(6); Cu1−N3, 1.923(6); Cu1−N4, 2.015(6); Cu1−O2, 1.921(5); Cu1−O3, 2.611(5); N1−Cu1−N4, 146.1(3); N3−Cu1−O2, 166.8(3). Selected bond distances (Å) and angles (deg) for $\mathbf{L^2CuCl}$: Cu1−N1, 2.044(2); Cu1−N3, 1.914(2); Cu1−N4, 2.002(2); Cu1−O2, 1.9500(17); Cu1−O3, 2.3296(18); N1−Cu1−N4, 141.48(8); N3−Cu1−O2, 167.67(8).

The complexes also were characterized by EPR spectroscopy (Figure S38), and the data show pseudoaxial signals with some degree of rhombicity as evidenced by the simulated *g*-values (Table S3), indicative of tetragonal Cu(II) complexes. Cu hyperfine and N superhyperfine couplings are observed in both spectra (parameters listed in Table S3). The UV−vis spectra for $\mathbf{L^1CuOAc}$ and $\mathbf{L^2CuOAc}$ in MeCN (Figure S20) have peaks at 694 nm (ε = 208 M^{-1} cm^{-1}) and 694 nm (ε = 292 M^{-1} cm^{-1}), respectively, typical for *d*-*d* transitions of Cu(II) complexes but different than the features found for $\mathbf{L^1CuCl}$, $\mathbf{L^2CuCl}$, [$\mathbf{L^1CuMeCN}$][SbF_6], and [$\mathbf{L^2CuMeCN}$][SbF_6].

Cu(II)−Cl Complex Bearing $(L^3)^-$. Attempts to make a Cu(I) complex with $\mathbf{HL^3}$ afforded a very poorly soluble orange material, which appeared similarly unreactive toward oxygen as $(\mathbf{L^2Cu})_2$ but was problematic to characterize. We therefore focused efforts on preparing Cu(II) complexes instead. The chloro complex $\mathbf{L^3CuCl}$ was obtained via direct reaction between $\mathbf{HL^3}$, $CuCl_2$, and NEt_3, affording a brown-green species in 85% yield. The crystal structure (Figure 7) indicates a mononuclear complex with distorted square planar geometry (τ_4 = 0.40) and typical Cu−L bond lengths for Cu(II). The distortion in geometry is likely in large part due to the ligand's unequal bite angles and nonplanar conformation and is similar to the structure we observed for $\mathbf{L^1CuCl}$. EPR spectroscopy in CH_2Cl_2 at 30 K (Figure S39; simulated parameters in Table S4) shows a broad and mostly featureless resonance, save for some faint Cu hyperfine interactions. The origin of this broadness is unclear.

Cu(II)−Solvento Complex Bearing $(L^3)^-$. The solvento adduct [$\mathbf{L^3CuMeCN}$][SbF_6] was produced by reacting $\mathbf{HL^3}$,

https://doi.org/10.1021/acsomega.2c04432
ACS Omega 2022, 7, 35217−35232

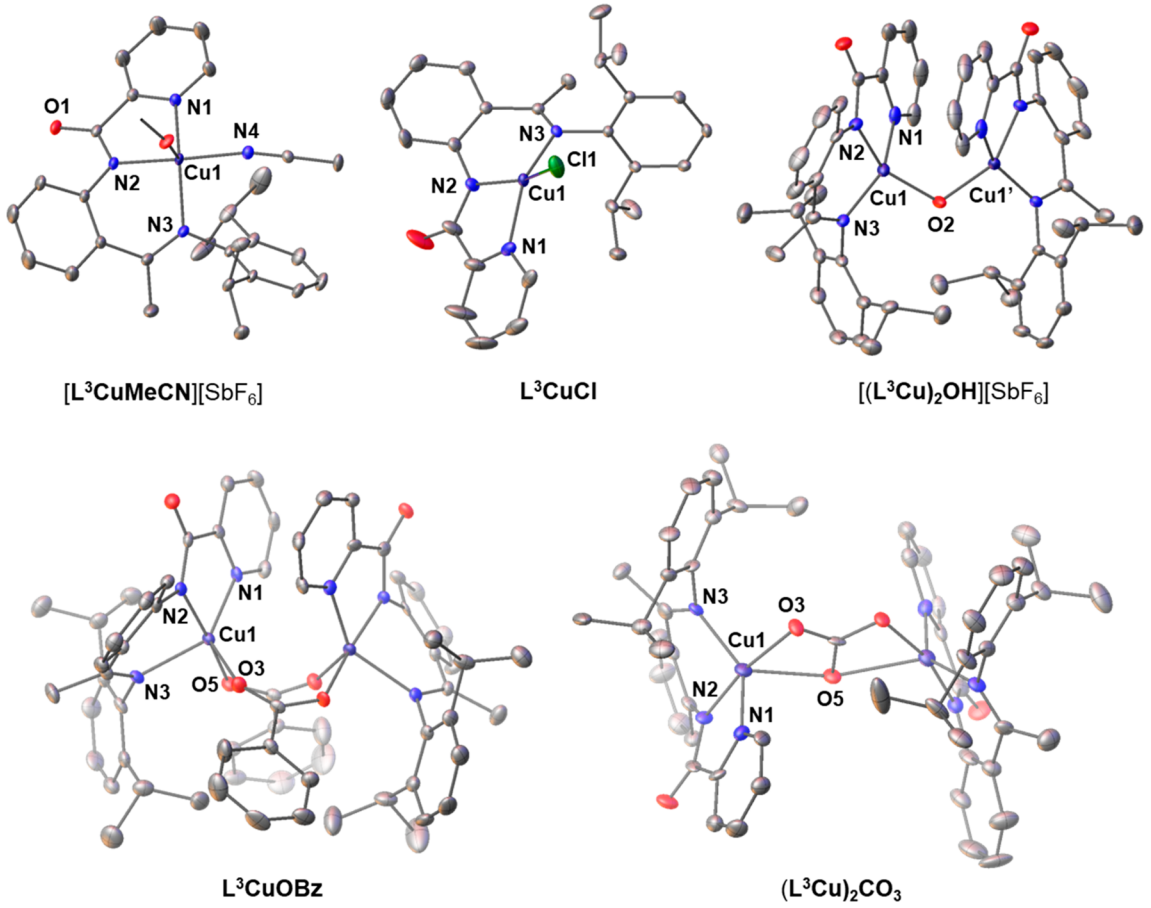

Figure 7. Crystal structures of the Cu(II) complexes bearing $\mathbf{L^3}$, drawn at the 50% probability level. Hydrogen atoms, counterions, and solvent molecules omitted for clarity. Selected bond distances (Å) and angles (deg) for [$\mathbf{L^3CuMeCN}$][$\mathbf{SbF_6}$]: Cu1−N1, 2.021(2); Cu1−N2, 1.926(2); Cu1−N3, 2.0514(19); Cu1−N4, 1.988(2); Cu1−O1, 2.199(2); N1−Cu1−N3, 144.20(7); N2−Cu1−N4, 175.07(8). Selected bond distances (Å) and angles (deg) for $\mathbf{L^3CuCl}$: Cu1−N1, 1.995(2); Cu1−N2, 1.912(2); Cu1−N3, 1.989(2); Cu1−Cl1, 2.2113(7); N1−Cu1−N3, 155.85(7); N2−Cu1−Cl1, 147.65(8). Selected bond distances (Å) and angles (deg) for [$\mathbf{(L^3Cu)_2OH}$][$\mathbf{SbF_6}$]: Cu1−N1, 1.9819(17); Cu1−N2, 1.9088(16); Cu1−N3, 1.9466(16); Cu1−O2, 1.9182(11); N1−Cu1−N3, 150.07(6); N2−Cu1−O2, 147.18(6); Cu1−O2−Cu1′, 115.16(11). Selected bond distances (Å) and angles (deg) for $\mathbf{L^3CuOBz}$ (averaged): Cu1−N1, 2.043(3); Cu1−N2, 1.929(3); Cu1−N3, 2.120(3); Cu1−O3, 1.922(3); Cu1−O5, 2.131(3); N1−Cu1−N3, 136.98(12); N2−Cu1−O3, 171.14(12); N1−Cu1−O5, 130.68(11). Selected bond distances (Å) and angles (deg) for $\mathbf{(L^3Cu)_2CO_3}$ (averaged): Cu1−N1, 2.034(5); Cu1−N2, 1.904(5); Cu1−N3, 2.020(5); Cu1−O3, 1.921(4); Cu1−O5, 2.131(3); N1−Cu1−N3, 139.54(12); N2−Cu1−O3, 166.29(19); N1−Cu1−O5, 98.04(16).

$[Cu(MeCN)_5][SbF_6]_2$, and NEt_3, affording the dark green complex in 78% yield. The structure of [$\mathbf{L^3CuMeCN}$][$\mathbf{SbF_6}$] (Figure 7) is analogous to that of $\mathbf{L^3CuCl}$, but with axial coordination of a neighboring complex's carbonyl group (2.20 Å bond length), resulting in a distorted square pyramidal (τ_5 = 0.35) coordination polymer (Figure S35). We speculate that this behavior is the result of a more electrophilic metal center than in the case of $\mathbf{L^3CuCl}$, and we note that it has been seen in other Cu(II) complexes with carbonyl-containing ligands.[41,43] The coordination polymer does not appear to persist in solution, as we observe a typical pseudoaxial monomeric Cu(II) EPR signal for the compound in THF at 30 K (Figure S39; simulated parameters in Table S5). UV−visible spectroscopy of both complexes in CH_2Cl_2 (Figures S17, S19) revealed weakly absorbing peaks in the visible region: 700 nm (260 M^{-1} cm^{-1}) for [$\mathbf{L^3CuMeCN}$][$\mathbf{SbF_6}$] and 566 nm (150 M^{-1} cm^{-1}) and 760 nm (140 M^{-1} cm^{-1}) for $\mathbf{L^3CuCl}$, typical values for Cu(II) d−d transitions.

***μ*-Hydroxo−Dicopper Complex.** Seeking to prepare Cu−O species, we targeted a hydroxo complex via reaction between [$\mathbf{L^3CuMeCN}$][$\mathbf{SbF_6}$] and NBu_4OH under inert atmosphere, which resulted in the formation of a red substance which could not be characterized. We then attempted to obtain the aquo complex by treating [$\mathbf{L^3CuMeCN}$][$\mathbf{SbF_6}$] with water, but this unexpectedly led to the formation of a μ-hydroxo dimer, [$\mathbf{(L^3Cu)_2OH}$][$\mathbf{SbF_6}$], a brown compound isolated in 54% yield. The crystal structure (Figure 7) indicates bond lengths typical for Cu(II) (e.g., Cu−OH bond length of 1.915 Å). A Cu−O−Cu bond angle of 115.5°, a prominent residual electron density peak at the cusp of the O atom, and the presence of one counterion per dimer reveal that the bridging moiety is a hydroxo rather than an oxo group. Similar to the monomeric complexes, the local geometry around each metal center is significantly distorted square planar (τ_4 = 0.45). UV−visible spectroscopy in CH_2Cl_2 (Figure S21) shows a peak at 534 nm (300 M^{-1} cm^{-1}) and a shoulder feature at 747 nm (130 M^{-1} cm^{-1}), consistent with d−d Cu(II) transitions. The absence of an EPR signal in frozen CH_2Cl_2 solution at 30 K (Figure S39) suggests that the dimer persists in solution and has an S = 0 ground state due to antiferromagnetic coupling of the unpaired spins. Such μ-hydroxo−dicopper(II) cores have been reported, with fairly wide-ranging bond metrics (reported

https://doi.org/10.1021/acsomega.2c04432
ACS Omega 2022, 7, 35217−35232

Cu−OH bond lengths range in excess of 1.9−2.2 Å).[92−112] The spontaneous formation of a hydroxo moiety likely occurs due to electronic deficiency in the ligand set of $[\mathbf{L^3CuMeCN}]^+$ rendering the Cu center Lewis acidic; the incomplete yield and observed formation of a pale blue aqueous fraction during preparation (see Experimental section) suggests partial demetalation, releasing the ligand's basic groups to facilitate the deprotonation.

Cu(II)−Benzoate Complex Bearing $(\mathbf{L^3})^-$. We also targeted the formation of a carboxylate complex by reacting $[\mathbf{L^3CuMeCN}][SbF_6]$ with sodium benzoate; this resulted in the bright green compound $\mathbf{L^3CuOBz}$ that crystallizes as a five-coordinate dimer (Figure 7) in 79% yield. In the solid state, two benzoate moieties bridge between the two Cu centers via each O atom, with prominent Jahn−Teller asymmetry between the two Cu−O bonds (avg 1.92 Å vs 2.13 Å), analogous to the Cu−Cl interactions in the dimeric solid state structure of $\mathbf{L^2CuCl}$. The local geometry at each Cu center is intermediate between square pyramidal and trigonal bipyramidal, leaning toward the latter (τ_5 = 0.57). On the other hand, we observed a typical square planar, pseudoaxial Cu(II) EPR signal in frozen CH_2Cl_2 solution at 30 K (Figure S39; simulated parameters in Table S6), indicating that a monomeric state, most likely with κ^1-coordinated benzoate, predominates in solution. UV−visible spectroscopy in CH_2Cl_2 (Figure S22) reveals one weakly absorbing peak in the visible region at 666 nm (220 M^{-1} cm^{-1}) consistent with the Cu(II) d−d transition. Numerous examples of both mononuclear and carboxylate-bridged dimers of Cu exist in the literature.[45,112−115]

Carbonate-Bridged Dicopper Complex. During our various metalation trials of $\mathbf{HL^3}$ with Cu(II), we observed that use of strong bases during the process, such as NaOH or NaOMe, led to formation of a bright green compound if ambient air was introduced into the reaction mixtures. The UV−visible spectrum of the green compound in CH_2Cl_2 (Figure S23) indicated a typical Cu(II) complex with a feature in the visible region at 679 nm (280 M^{-1} cm^{-1}). Isolation and crystallization revealed this compound to be a carbonate-bridged dimer, $\mathbf{(L^3Cu)_2CO_3}$ (Figure 7), with each Cu center coordinating strongly to one O atom (avg bond length 1.92 Å) equatorially, and both interacting more weakly with the third O atom (avg bond length 2.41 Å) mostly aligned to the Jahn−Teller axis, giving a local coordination that is distorted square pyramidal (τ_5 = 0.25). EPR spectroscopy in frozen CH_2Cl_2 (Figure S39) revealed no signal, consistent with retention of the dimeric structure in solution. The route of formation of this species is most likely capture of atmospheric CO_2, either by the utilized bases themselves or some intermediate basic Cu species. We readily synthesized the same dimer by direct metalation using $\mathbf{HL^3}$, anhydrous $CuCl_2$, and K_2CO_3, in 93% yield. Copper(II) dimers bridged by carbonate in this manner are known in the literature and exhibit similar bond lengths.[116−123]

Electrochemistry. We investigated the accessibility of additional oxidation states using cyclic voltammetry in the 11 Cu(II) complexes: $\mathbf{L^1CuCl}$, $\mathbf{L^2CuCl}$, $[\mathbf{L^1CuMeCN}][SbF_6]$, $[\mathbf{L^2CuMeCN}][SbF_6]$, $\mathbf{L^1CuOAc}$, and $\mathbf{L^2CuOAc}$ in MeCN solutions and $[\mathbf{L^3CuMeCN}][SbF_6]$, $\mathbf{L^3CuCl}$, $[(\mathbf{L^3Cu})_2\mathbf{OH}][SbF_6]$, $\mathbf{L^3CuOBz}$, and $\mathbf{(L^3Cu)_2CO_3}$ in CH_2Cl_2 solutions (Figures S25−S30). No reversible oxidation or reduction events were observed for any of the compounds, with several irregular irreversible oxidative features starting in the vicinity of 0.7−1 V vs Fc^+/Fc, most consistent with oxidative degradation of the compounds. We therefore conclude that highly oxidized Cu complexes supported by $(\mathbf{L^n})^-$ (n = 1, 2, or 3) are not feasible species to access due to their apparent instabilities. Irreversible reductive features are observed below −0.2 V vs Fc^+/Fc, and based on our Cu(I) metalation experiments, we suspect that these most likely correspond to Cu(I) reduction accompanied by extensive coordinative rearrangement to form dimeric or polymeric aggregates like $\mathbf{(L^2Cu)_2}$.

Attempted Synthesis of Copper-Superoxide Species. Since neither the Cu(I) nor Cu(III) states were accessible for reactivity studies, we sought to produce mononuclear Cu(II)−oxygen species via reaction of Cu(II) complexes with superoxide. In a method analogous to that used in previous work with pyridine(dicarboxamide) systems,[29,34] we reacted $[\mathbf{L^nCuMeCN}][SbF_6]$ ($\mathbf{n}$ = 1−3) with $[K(Krypt)][O_2]$ in THF at −80 °C. Unfortunately, we did not observe the formation of spectroscopic features indicative of $Cu-O_2$ species upon addition of the superoxide salt to the Cu(II) complexes under these conditions (Figures S31−S33). Additionally, we did not witness any hydrogen atom transfer reactivity with substrates like TEMPOH or 9,10-dihydroanthracene with the solutions comprising $[\mathbf{L^3CuMeCN}][SbF_6]$ + $[K(Krypt)][O_2]$.

CONCLUSIONS

We prepared three new monoanionic N,N',N'' ligands with a central anionic amido coordinating group flanked by two neutral N donors in an effort to examine in model complexes the effects of a single negative charge as debated for the LPMO active site. A Cu(I) dimer ligated by $^-\mathbf{L^2}$ was isolated from an attempt to synthesize a mononuclear Cu(I) complex. Attempts to form a 1:1 Cu/O_2 complex by reacting $\mathbf{(L^2Cu)_2}$ with O_2 were not successful. The monoanionic supporting ligands bind Cu(II) in a tridentate pincer fashion, affording a number of Cu(II) complexes in which a variety of neutral or anionic auxiliary ligands could be installed at the fourth and sometimes fifth coordination site, resulting in geometries for some of the monocopper(II) complexes that resemble those of the Cu(II) resting state of LPMO. Depending on the nature of the auxiliary ligands, we obtained mononuclear, dinuclear, and fluxional species. The challenges we faced with both obtaining copper−oxygen species as well as oxidizing these compounds to a formally Cu(III) state prevented us from studying substrate oxidation reactivity with $[Cu\text{-}OR]^{2+}$-type species. While we had hoped that the lower donor strength of these ligands would lend access to O_2-reactive Cu(I) species, the lack of which is a major drawback of the pyridine dicarboxamide ligand framework, we observed a tendency to form an unreactive dimer. We speculate this may be due to a steric insufficiency or high flexibility in the explored ligands. Bulkier modifications to these frameworks could alleviate this issue and would be reasonable targets for further investigation. Nonetheless, the ligands presented in this work give access to a relatively unexplored coordination environment for Cu and could be useful in other lines of coordination chemistry research.

EXPERIMENTAL SECTION

Materials and Methods. All air-sensitive manipulations were carried out in a dinitrogen-filled glovebox or under argon using Schlenk techniques. All reagents and solvents were purchased from commercial vendors and used as received unless otherwise noted. Tetrahydrofuran, dichloromethane,

https://doi.org/10.1021/acsomega.2c04432
ACS Omega 2022, 7, 35217−35232

acetonitrile, pentane, diethyl ether, and heptane were passed through activated alumina columns and used directly or plumbed into a glovebox. Tetrahydrofuran, dichloromethane, and acetonitrile were stored over activated 3 Å molecular sieves in a dinitrogen-filled glovebox and, prior to use in spectroscopy and cyclic voltammetry experiments, filtered using a 25 mm diameter, 0.2 mm hydrophobic polytetrafluoroethylene (PTFE) syringe filter. 3,5-Diisopropylpyrazole was either made according to the previously published synthesis[124] or purchased from Tokyo Chemical Industry Co., Ltd. and used without further purification. KHMDS was purchased from Sigma-Aldrich and was recrystallized from toluene at −35 °C, filtered, and dried *in vacuo* before use. $Cu(MeCN)_4OTf$,[125] $[Cu(MeCN)_5][SbF_6]_2$,[126] and *N*-(2-acetylphenyl)-picolinamide[71] were made according to the previously published syntheses. 3,5-Dimethylpyrazole, 1-fluoro-2-nitrobenzene, picolinic acid, and anhydrous $CuCl_2$ were purchased from Sigma-Aldrich and used without further purification.

UV−vis spectra were collected using a HP8453 (190−1100 nm) diode array spectrophotometer equipped with a Unisoku low-temperature UV−vis cell holder. EPR spectra were collected on frozen 1 mM samples with a CW Elexsys E500 EPR spectrometer using X band (9.38 GHz) radiation at 35 dB and 30 K with the following conditions: microwave power, 0.0002 mW; modulation amplitude, 9.6 G; and modulation frequency, 100 kHz. EPR spectra were simulated using the EasySpin EPR simulation package, v. 5.1.[127] NMR spectra were collected on a Bruker Avance III HD nanobay AX-400, a Bruker Avance III HD-500, or an Agilent DD2 (500 MHz) spectrometer. Deuterated tetrahydrofuran was purchased from Cambridge Isotopes Laboratories, degassed, and dried over 3 Å molecular sieves prior to use. Cyclic voltammograms were recorded using an EC Epsilon potentiostat from BASi, a glassy carbon working electrode, and a Ag wire pseudoreference electrode. All cyclic voltammograms were performed in THF or MeCN with 0.3 M tetrabutylammonium hexafluorophosphate (TBAP) electrolyte, which was recrystallized several times from ethanol and dried under high vacuum before use and were internally referenced to the ferrocene/ferrocenium (Fc/Fc^+) couple. The spectra were converted vs the standard Fc/Fc^+ couple using standard conversion factors.[128] Elemental analysis was performed by the CENTC Elemental Analysis Facility (University of Rochester). ESI-HR-MS data is supplied by instruments funded by NIH grant 8P41GM103422.

For X-ray crystallography experiments, crystals were placed onto the tip of a MiTeGen cryoloop and mounted on a Bruker D8 VENTURE diffactometer equipped with a Photon III CMOS and a Mo Kα source using normal parabolic mirrors as monochromators or a Bruker X8 diffractometer equipped with a Kappa Apex II CCD using a graphite monochromator, with the crystals cooled to 100 K in a nitrogen stream. Data collection and processing were performed within the Bruker APEX3[129] software suite, using SAINT[129] for data reduction and SADABS[130] for scaling an absorption correction. Structure solutions were performed with SHELXT[131] or SHELXS[132] using OLEX 2[133] or ShelXle[134] as graphical interfaces. The structures were refined against F^2 on all data by full matrix least-squares with SHELXL.[132]

3,5-Dimethyl-1-(2-nitrophenyl)-1*H*-pyrazole. The following preparation was adapted from a previously published synthesis.[70] Under an argon atmosphere, a flame-dried 500 mL Schlenk flask containing dry THF (100 mL) was charged with NaH (60% in mineral oil, 1.931 g, 48.3 mmol) and then cooled to 0 °C using an ice bath. The slurry was stirred while a solution of 3,5-dimethylpyrazole (5.00 g, 52.0 mmol) in dry THF (100 mL) was added dropwise via an addition funnel over 30 min. After the addition was complete, a solution of 1-fluoro-2-nitrobenzene (5.49 mL, 7.339 g, 52.0 mmol) in dry THF (100 mL) was added dropwise via an addition funnel over 30 min. The ice bath was removed, and the orange solution was allowed to stir at rt for 2 h under argon. The reaction was transferred to a separatory funnel and slowly quenched with a saturated aqueous NH_4Cl solution (100 mL). After separation of the phases, the aqueous layer was extracted with ethyl acetate (2 × 200 mL). The organic layers were combined, washed with brine (50 mL), dried with Na_2SO_4, and decanted, and the solvents were removed *in vacuo*. The resulting orange residue was purified via column chromatography on silica gel (50% CH_2Cl_2, 50% ethyl acetate) affording the pure product as an orange oil (8.209 g, 73% yield). ^1H NMR (500 MHz, $CDCl_3$) δ (ppm): 7.93 (dd, J = 8.1, 1.5 Hz, 1H), 7.66 (td, J = 7.8, 1.5 Hz, 1H), 7.53 (td, J = 7.8, 1.4 Hz, 1H), 7.45 (dd, J = 7.9, 1.4 Hz, 1H), 5.99 (s, 1H), 2.21 (s, 3H), 2.15 (s, 3H). ^{13}C NMR (500 MHz, $CDCl_3$) δ (ppm): 150.67, 146.59, 141.09, 133.37, 133.29, 129.67, 129.34, 125.25, 107.00, 13.64, 11.49. Anal. Calcd for $C_{11}H_{11}N_3O_2$: C 60.82, H 5.1, N 19.34. Found: C 60.57, H 5.15, N 19.02.

3,5-Diisopropyl-1-(2-nitrophenyl)-1*H*-pyrazole. The following preparation was adapted from a previously published synthesis.[70] Under an argon atmosphere, a flame-dried 500 mL Schlenk flask containing dry THF (100 mL) was charged with NaH (60% in mineral oil, 3.941 g, 104.5 mmol) then cooled to 0 °C using an ice bath. The slurry was stirred while a solution of 3,5-diisopropylpyrazole (10.00 g, 65.7 mmol) in dry THF (100 mL) was added dropwise via an addition funnel over 30 min. After the addition was complete, a solution of 1-fluoro-2-nitrobenzene (6.93 mL, 9.268 g, 65.7 mmol) in dry THF (100 mL) was added dropwise via an addition funnel over 30 min. The ice bath was removed, and the orange solution was allowed to stir at rt for 2 h under argon. The reaction was transferred to a separatory funnel and slowly quenched with a saturated aqueous NH_4Cl solution (150 mL). After separation of the phases, the aqueous layer was extracted with ethyl acetate (2 × 200 mL). The organic layers were combined, washed with brine (50 mL), dried with Na_2SO_4, and decanted, and the solvents were removed *in vacuo*. The resulting orange residue was purified via column chromatography on silica gel (80% hexanes, 20% ethyl acetate) affording the pure product as an orange oil (10.735 g, 66% yield). ^1H NMR (400 MHz, $CDCl_3$) δ (ppm): 7.97 (dd, J = 8.1, 1.5 Hz, 1H), 7.68 (td, J = 7.7, 1.2 Hz, 1H), 7.56 (td, J = 7.9, 1.2 Hz, 1H), 7.51 (dd, J = 8.0, 1.2 Hz, 1H), 6.06 (s, 1H), 2.94 (sept, J = 6.9 Hz, 1H), 2.81 (sept, J = 6.9 Hz, 1H), 1.25 (d, J = 6.9 Hz, 6H), 1.18 (d, J = 6.9 Hz, 6H). ^{13}C NMR (500 MHz, $CDCl_3$) δ (ppm): 161.04, 151.91, 146.90, 133.77, 133.09, 129.60, 129.32, 125.35, 100.39, 28.09, 25.77, 22.85, 22.80. Anal. Calcd for $C_{15}H_{19}N_3O_2$: C 65.91, H 7.01, N 15.37. Found: C 66.09, H 7.23, N 15.27.

2-(3,5-Dimethyl-1*H*-pyrazol-1-yl)aniline. The following preparation was adapted from a previously published synthesis.[70] Under argon, a Schlenk flask was charged with 3,5-dimethyl-1-(2-nitrophenyl)-1*H*-pyrazole (8.097 g, 37.3 mmol), 10 wt % Pd/C (0.282 g, 0.265 mmol), and 200 proof ethanol (50 mL). The flask was flushed with H_2 then stirred at rt for 24 h under a balloon of H_2, refilling the H_2 balloon when deflated. The reaction mixture was filtered through Celite, and the solids were washed with ethanol (50 mL). *Note: Residual Pd/C should*

https://doi.org/10.1021/acsomega.2c04432
ACS Omega 2022, 7, 35217−35232

be wetted with water after filtration to prevent ignition of the solid. Solvent was removed *in vacuo* yielding the pure product as a brown solid (6.609 g, 95% yield). ^{1}H NMR (400 MHz, $CDCl_3$) δ (ppm): 7.13 (ddd, J = 8.1, 7.3, 1.6 Hz, 1H), 7.04 (dd, J = 7.6, 1.6 Hz, 1H), 6.78−6.68 (m, 2H), 5.95 (s, 1H), 3.77 (s, 2H), 2.26 (s, 3H), 2.11 (s, 3H). ^{13}C NMR (500 MHz, $CDCl_3$) δ (ppm): 149.52, 143.52, 140.85, 129.52, 127.68, 125.62, 118.15, 116.73, 105.75, 13.75, 11.62. Anal. Calcd for $C_{11}H_{13}N_3$: C 70.56, H 7.00, N 22.44. Found: C 70.56, H 7.09, N 22.37.

2-(3,5-Diisopropyl-1*H*-pyrazol-1-yl)aniline. The following preparation was adapted from a previously published synthesis.[70] Under argon, a Fisher Porter tube was charged with 3,5-diisopropyl-1-(2-nitrophenyl)-1*H*-pyrazole (2.264 g, 8.28 mmol), 10 wt % Pd/C (0.063 g, 0.059 mmol), and 200 proof ethanol (15 mL). The system was sealed and flushed with H_2 through three pressurization/vent cycles then pressurized once more to 100 psi H_2 and stirred at rt overnight. The vessel was repressurized once during the reaction. *Note: A safety shield should be placed in front of the Fisher Porter tube during this reaction.* Residual pressure in the vessel was vented before filtering the reaction mixture through Celite and washing the solids with ethanol (15 mL). *Note: Residual Pd/C should be wetted with water after filtration to prevent ignition of the solid.* Solvent was removed *in vacuo* to yield the product as a white solid (1.876 g, 93% yield). ^{1}H NMR (400 MHz, $CDCl_3$): δ_H 7.18 (ddd, J = 8.1, 7.3, 1.5 Hz, 1H), 7.11 (dd, J = 7.8, 1.5 Hz, 1H), 6.78 (m, 2H), 6.02 (s, 1H), 3.83 (s, 2H), 3.00 (sept, J = 6.9 Hz, 1H), 2.83 (sept, J = 6.9 Hz, 1H), 1.29 (d, J = 6.9 Hz, 6H), 1.14 (d, J = 6.9 Hz, 6H). ^{13}C NMR (500 MHz, $CDCl_3$) δ (ppm): 160.08, 151.75, 144.00, 129.66, 128.00, 126.01, 118.15, 116.74, 99.02, 28.15, 25.60, 23.01, 22.82. Anal. Calcd for $C_{15}H_{21}N_3$: C 74.03, H 8.70, N 17.27. Found: C 74.54, H 8.93, N 17.40.

***N*-(2-(3,5-Dimethyl-1*H*-pyrazol-1-yl)phenyl)-picolinamide (HL^1).** The following preparation was adapted from a previously published synthesis.[70] In a 250 mL Schlenk flask under argon, a solution of picolinic acid (3.117 g, 25.3 mmol) in CH_2Cl_2 (35 mL) was cooled to 0 °C using an ice bath. With stirring, DMF (5 drops) was added dropwise to the solution, followed by another dropwise addition of oxalyl chloride (2.96 mL, 34.5 mmol). The purple solution was brought to rt and stirred for 1 h. The solvent and excess oxalyl chloride were removed *in vacuo* to yield the acid chloride as a dark black/brown oily solid. *Note: the excess oxalyl chloride was collected in an external trap to be quenched with a saturated aqueous solution of sodium bicarbonate.* To the same flask under argon, the acid chloride was dissolved in CH_2Cl_2 (35 mL) and cooled back to 0 °C using an ice bath. A solution of 2-(3,5-dimethyl-1*H*-pyrazol-1-yl)aniline (4.310 g, 23.0 mmol) in CH_2Cl_2 (35 mL) was added to the flask, followed by the addition of triethylamine (3.53 mL, 25.3 mmol). The flask was removed from the ice bath, and the reaction was stirred at rt for 12 h. The reaction mixture was filtered into a separatory funnel and washed with a saturated aqueous ammonium chloride solution (2 × 20 mL) and brine (30 mL). The organic layer was dried with Na_2SO_4, decanted, and then concentrated *in vacuo*. The crude product was purified by via column chromatography on silica gel (90% hexanes, 10% ethyl acetate;) affording the pure product as an yellow/orange oil (5.686 g, 85% yield). Over a few months, the oil solidified into a brown solid. ^{1}H NMR (400 MHz, $CDCl_3$): δ_H 11.11 (s, 1H), 8.69 (dd, J = 8.3, 1.4 Hz, 1H), 8.52 (ddd, J = 4.8, 1.7, 1.0 Hz, 1H), 8.21 (dt, J = 7.9, 1.1 Hz, 1H), 7.83 (td, J = 7.7, 1.7 Hz, 1H), 7.45 (ddd, J = 8.6, 7.6, 1.6 Hz, 1H), 7.40 (ddd, J = 7.6, 4.7, 1.2 Hz, 1H), 7.28 (dd, J = 7.9, 1.6 Hz, 1H), 7.19 (td, J = 7.7, 1.4 Hz, 1H), 6.06 (s, 1H), 2.43 (s, 3H), 2.19 (s, 3H). ^{13}C NMR (500 MHz, $CDCl_3$) δ (ppm): 162.65, 150.31, 150.13, 148.28, 141.24, 137.48, 134.46, 129.22, 129.19, 126.52, 126.38, 123.75, 122.46, 121.89, 106.71, 13.72, 12.01. Anal. Calcd for $C_{17}H_{16}N_4O$: C 69.85, H 5.52, N 19.17. Found: C 69.64, H 5.52, N 19.17.

***N*-(2-(3,5-Diisopropyl-1*H*-pyrazol-1-yl)phenyl)-picolinamide (HL^2).** The following preparation was adapted from a previously published synthesis.[70] In a 100 mL Schlenk flask under argon, a solution of picolinic acid (2.230 g, 18.1 mmol) in CH_2Cl_2 (25 mL) was cooled to 0 °C using an ice bath. With stirring, DMF (5 drops) was added dropwise to the solution, followed by another dropwise addition of oxalyl chloride (2.11 mL, 24.7 mmol). The purple solution was brought to rt and stirred for 1 h. The solvent and excess oxalyl chloride were removed *in vacuo* to yield the acid chloride as a dark black/brown oily solid. *Note: the excess oxalyl chloride was collected in an external trap to be quenched with a saturated aqueous solution of sodium bicarbonate.* To the same flask under argon, the acid chloride was dissolved in CH_2Cl_2 (25 mL) and cooled back to 0 °C using an ice bath. A solution of 2-(3,5-diisopropyl-1*H*-pyrazol-1-yl)aniline (4.000 g, 16.4 mmol) in CH_2Cl_2 (25 mL) was added to the flask, followed by the addition of triethylamine (2.52 mL, 18.1 mmol). The flask was removed from the ice bath, and the reaction was stirred at rt for 12 h. The reaction mixture was filtered into a separatory funnel and washed with a saturated aqueous ammonium chloride solution (2 × 10 mL) and brine (20 mL). The organic layer was dried with Na_2SO_4, decanted, and then concentrated *in vacuo*. The crude product was purified by via column chromatography on silica gel (90% hexanes, 10% ethyl acetate) affording the pure product as a white solid (4.050 g, 71% yield). ^{1}H NMR (400 MHz, $CDCl_3$): δ_H 10.58 (s, 1H), 8.69 (dd, J = 8.3, 1.4 Hz, 1H), 8.46 (ddd, J = 4.8, 1.8, 1.0 Hz, 1H), 8.22 (dt, J = 7.9, 1.1 Hz, 1H), 7.83 (tt, J = 7.7, 1.7 Hz, 1H), 7.47 (td, J = 7.9, 1.5 Hz, 1H), 7.39 (ddt, J = 7.6, 4.8, 1.4 Hz, 1H), 7.33 (dd, J = 7.8, 1.6 Hz, 1H), 7.19 (td, J = 7.6, 1.3 Hz, 1H), 6.10 (s, 1H), 3.12 (sept, J = 7.0 Hz, 1H), 2.85 (sept, J = 6.8 Hz, 1H), 1.40 (d, J = 7.0 Hz, 6H), 1.09 (d, J = 6.9 Hz, 6H). ^{13}C NMR (500 MHz, $CDCl_3$) δ (ppm): 162.61, 160.77, 152.30, 149.96, 148.10, 137.42, 135.17, 129.68, 129.58, 127.23, 126.40, 123.89, 122.47, 121.94, 99.92, 28.32, 25.62, 22.95, 22.83. Anal. Calcd for $C_{21}H_{24}N_4O$: C 72.39, H 6.94, N 16.08. Found: C 72.41, H 7.20, N 15.95.

***N*-(2-(1-((2,6-Diisopropylphenyl)imino)ethyl)phenyl)-picolinamide (HL^3).** In a flame-dried 250 mL Schlenk flask under argon, 2,6-bis(isopropyl)aniline (5.6 mL, 30 mmol) was dissolved in 150 mL of dry, degassed toluene and cooled in an ice−water bath. Titanium tetrachloride (0.55 mL, 5.0 mmol) was added dropwise with stirring, resulting in the formation of a red solution progressing to a brown suspension over the course of the addition. After stirring for 1 h, the reaction was warmed to room temperature, and *N*-(2-acetylphenyl)-picolinamide (2.39 g, 10 mmol) was added, after which the reaction was heated to reflux for 48 h. The crude mixture was washed with saturated aqueous K_2CO_3, and the organic fraction was concentrated under reduced pressure. The majority of unreacted picolinamide starting material was removed by extracting the evaporated residue with pentane and passing through a filter. The resulting filtrate was again

https://doi.org/10.1021/acsomega.2c04432
ACS Omega 2022, 7, 35217−35232

concentrated under reduced pressure and loaded onto a silica gel column presoaked in hexanes (4 × 20 cm) using a minimal amount of pentane. Separation was carried out using an autocolumn eluting with a gradient solvent mixture starting at 25% CH_2Cl_2 in hexane and ramping to 100% CH_2Cl_2 over 5 column volumes. The desired product was the second major fraction, eluting at approximately 66% CH_2Cl_2 (first was 2,6-bis(isopropyl)aniline, at approximately 33% CH_2Cl_2). The product was concentrated under reduced pressure to a viscous yellow oil, which on standing under dynamic vacuum overnight afforded a glassy yellow residue. Final purification was carried out via recrystallization from a slowly evaporating concentrated pentane solution in the presence of seed crystals (initially obtained via prolonged standing in ambient air of a small amount of product in its oily state), affording light yellow crystalline material. Yield: 1.135 g, 29%. ^{1}H NMR (500 MHz, $CDCl_3$): δ_H (ppm) 15.38 (s, 1H), 9.16 (d, J = 8.3 Hz, 1H), 8.27 (d, J = 7.8 Hz, 1H), 8.09 (d, J = 4.5 Hz, 1H), 7.91 (d, J = 8.0 Hz, 1H), 7.83 (td, J = 7.7, 1.5 Hz, 1H), 7.61 (t, J = 7.8 Hz, 1H), 7.32−7.19 (m, 4H), 2.85 (sept, J = 6.9 Hz, 2H), 2.29 (s, 3H), 1.18 (d, J = 6.9 Hz, 6H), 1.01 (d, J = 6.8 Hz, 6H). ^{13}C NMR (500 MHz, $CDCl_3$): δ (ppm) 168.27, 164.60, 151.29, 148.30, 145.06, 140.60, 137.08, 136.71, 131.85, 130.14, 125.89, 124.06, 123.78, 123.00, 122.75, 122.51, 121.37, 28.55, 23.52, 22.96, 19.39. Anal. Calcd for $C_{26}H_{29}N_3O$: C 78.16, H 7.32, N 10.52. Found: C 78.41, H 7.46, N 10.57.

$(L^2Cu)_2$. In a glovebox, a solution of KHMDS (32 mg, 0.16 mmol) in MeCN (3 mL) was added dropwise to a solution of **HL^2** (50 mg, 0.14 mmol) in MeCN (2 mL) in a 20 mL scintillation vial while stirring. After complete addition of the base, a solution of $Cu(MeCN)_4OTf$ in MeCN (2 mL) was added dropwise to the vial with stirring, and a bright orange powder started to precipitate from the solution. After 10 min of stirring, the MeCN was decanted from the vial. The solid was rinsed with MeCN (2 × 3 mL), decanted, and dried *in vacuo* to afford the pure compound (39 mg, 33%). X-ray quality crystals (orange blocks) were formed upon slow diffusion of pentane into a concentrated THF solution of **$(L^2Cu^I)_2$** at −35 °C. ^{1}H NMR (400 MHz, THF-d_8): δ_H 7.80 (app d, J = 7.8 Hz, 1H), 7.57 (app t, J = 7.6 Hz, 1H), 7.45 (app d, J = 7.6 Hz, 1H), 7.32−7.11 (m, 4H), 7.01 (app t, J = 6.0 Hz, 1H), 5.91 (s, 1H), 3.27 (sept, J = 6.9 Hz, 1H), 3.09 (sept, J = 6.7 Hz, 1H), 1.38 (overlapping doublets, J = 6.8 Hz, 6H), 1.17 (d, J = 6.9 Hz, 3H), 0.47 (d, J = 6.9 Hz, 3H). ^{13}C NMR (500 MHz, THF-*d8*) δ (ppm): 166.47, 160.30, 155.27, 154.97, 152.93, 147.35, 137.85, 134.45, 130.23, 129.87, 128.06, 124.88, 123.24, 122.07, 97.65, 30.81, 30.39, 27.63, 24.50, 23.48, 22.67. UV−vis (THF, −80 °C) [λ_{max}, nm (ε, M^{-1} cm^{-1})]: 426 (16490), 592 (1365). Anal. Calcd for $C_{42}H_{46}Cu_2N_8O_2$: C 61.37, H 5.64, N 13.63. Found: C 60.83, H 5.62, N 13.29.

L^1CuCl. In a glovebox, a 50 mL Schlenk flask was charged with a solution of **HL^1** (111.2 mg, 0.38 mmol) in THF (4 mL). A solution of KHMDS (75.9 mg, 0.38 mmol) in THF (4 mL) was added dropwise to the flask with stirring. After complete addition of the base, a slurry of anhydrous $CuCl_2$ (49.1 mg, 0.37 mmol) in THF (4 mL) was added to the flask with stirring, producing a dark green reaction mixture. After stirring at rt for 30 min, the solvent and HMDS byproduct were removed *in vacuo*. CH_2Cl_2 (5 mL) was added to the flask, and the solution was filtered into a 20 mL scintillation vial using a 25 mm diameter, 0.2 mm hydrophobic PTFE syringe filter. The solvent was removed *in vacuo*. MeCN (5 mL) was used to dissolve the product and then filtered into a 20 mL scintillation vial using a 25 mm diameter, 0.2 mm hydrophobic PTFE syringe filter. The solvent was removed *in vacuo*, and the resulting green oil was triturated with diethyl ether (2 × 5 mL) resulting in a green powder (44.6 mg, 31%). Crystalline material of the title product was obtained by dissolving the green oil in a minimum amount of MeCN and layering with diethyl ether at rt, which afforded dark green plates that were suitable for X-ray diffraction. UV−vis (MeCN, 25 °C) [λ_{max}, nm (ε, M^{-1} cm^{-1})]: 463 (358), 604 (152), 775 (198). Anal. Calcd for $C_{17}H_{15}CuN_4OCl$: C 52.31, H 3.87, N 14.35. Found: C 54.18, H 4.13, N 14.61.

L^2CuCl. In a glovebox, a 50 mL Schlenk flask was charged with a solution of HL^2 (95.1 mg, 0.27 mmol) in THF (4 mL). A solution of KHMDS (54.4 mg, 0.27 mmol) in THF (4 mL) was added dropwise to the flask with stirring. After complete addition of the base, a slurry of anhydrous $CuCl_2$ (35.2 mg, 0.26 mmol) in THF (4 mL) was added to the flask with stirring, producing a dark green reaction mixture. After stirring at rt for 30 min, the solvent and HMDS byproduct were removed *in vacuo*. CH_2Cl_2 (5 mL) was added to the flask, and the solution was filtered into a 20 mL scintillation vial using a 25 mm diameter, 0.2 mm hydrophobic PTFE syringe filter. The solvent was removed *in vacuo*. MeCN (5 mL) was used to dissolve the product and then filtered into a 20 mL scintillation vial using a 25 mm diameter, 0.2 mm hydrophobic PTFE syringe filter. The solvent was removed *in vacuo*, and the resulting green oil was triturated with diethyl ether (2 × 5 mL) resulting in a green/brown powder (70.0 mg, 60%). Crystalline material of the title product was obtained by dissolving the green oil in a minimum amount of CH_2Cl_2 and layering with heptane at −20 °C, which resulted in an oil that was subsequently allowed to sit at rt overnight resulting in dark green plates that were suitable for X-ray diffraction. UV−vis (MeCN, 25 °C) [λ_{max}, nm (ε, M^{-1} cm^{-1})]: 458 (325), 606 (105), 815 (177). Anal. Calcd for $C_{21}H_{23}CuN_4OCl$: C 56.50, H 5.19, N 12.55. Found: C 57.02, H 5.24, N 12.53.

L^3CuCl. A 25 mL heart flask under ambient atmosphere was loaded with HL^3 (80 mg, 0.20 mmol), anhydrous $CuCl_2$ (27 mg, 0.20 mmol), and 4 mL of CH_2Cl_2 and then mixed until all ligand dissolved, giving a dull green solution along with some undissolved $CuCl_2$. Triethylamine (30 μL, 0.22 mmol) was added, and the solution was mixed with sonication until all $CuCl_2$ dissolved and a darker green hue developed (ca. 5 min). Pentane (ca. 9 mL) was added gradually with stirring, causing a pale precipitate (presumably $HNEt_3Cl$) to form, which was removed by filtration. The filtrate was concentrated under reduced pressure to a brown-green residue, redissolved in 1.5 mL of CH_2Cl_2 and layered with 18 mL of pentane, then allowed to stand undisturbed for 24 h. Dark brown crystals (suitable for diffractometry) were decanted and washed with pentane, then dried under vacuum overnight. Despite drying under reduced pressure, product was isolated as a solvated solid with 0.5 molecules of CH_2Cl_2 per [Cu]. Yield: 91.3 mg, 85%. Anal. Calcd for $C_{26}H_{28}ClCuN_3O + 0.5CH_2Cl_2$: C 58.94, H 5.41, N 7.78. Found: C 59.62, H 5.67, N 7.61. UV−vis (CH_2Cl_2, 25 °C): 233 nm (23000 M^{-1} cm^{-1}), 258 nm (25000 M^{-1} cm^{-1}), 365 nm (7800 M^{-1} cm^{-1}), 566 nm (150 M^{-1} cm^{-1}), 760 nm (140 M^{-1} cm^{-1}).

$[L^1Cu(MeCN)][SbF_6]$. In a glovebox, a 50 mL Schlenk flask was charged with a solution of **HL^1** (50 mg, 0.17 mmol) in MeCN (4 mL). A solution of KHMDS (34 mg, 0.17 mmol) in MeCN (4 mL) was added dropwise to the flask with stirring. After complete addition of the base, a solution of [**Cu-**

https://doi.org/10.1021/acsomega.2c04432
ACS Omega 2022, 7, 35217−35232

$(MeCN)_5][SbF_6]_2$ (122 mg, 0.16 mmol) in MeCN (4 mL) was added dropwise to the flask with stirring, producing a dark green reaction mixture. After stirring at rt for 30 min, the solvent and HMDS byproduct were removed *in vacuo*. The title product was obtained as a green solid after precipitating the compound out of MeCN (0.5 mL) with diethyl ether (10 mL) several times, decanting the liquid, and drying the solid *in vacuo* (108 mg, 104%). UV−vis (MeCN, 25 °C) [λ_{max}, nm (ε, M^{-1} cm^{-1})]: 466 (390), 731 (220). HR-MS (ESI, acetonitrile, positive ion) *m*/*z*: $[L^1Cu + SbF_6 + H]^+$ Calcd For $[C_{17}H_{16}CuN_4OSbF_6]^+$ (without acetonitrile) 591.96; Found 591.9591. Anal. Calcd for $C_{19}H_{18}CuN_5OSbF_6$ (with acetonitrile): C 36.13, H 2.87, N 11.09. Found: C 38.18, H 3.32, N 10.77.

[L^2Cu(MeCN)][SbF_6]. In a glovebox, a 50 mL Schlenk flask was charged with a solution of HL^2 (50 mg, 0.14 mmol) in MeCN (4 mL). A solution of KHMDS (29 mg, 0.14 mmol) in MeCN (4 mL) was added dropwise to the flask with stirring. After complete addition of the base, a solution of $[Cu(MeCN)_5][SbF_6]_2$ (102 mg, 0.14 mmol) in MeCN (4 mL) was added dropwise to the flask with stirring, producing a dark green reaction mixture. After stirring at rt for 30 min, the solvent and HMDS byproduct were removed *in vacuo*. The title product was obtained as a green solid after precipitating the compound out of MeCN (0.5 mL) with diethyl ether (10 mL) several times, decanting the liquid, and drying the solid *in vacuo* (89 mg, 94%). UV−vis (MeCN, 25 °C) [λ_{max}, nm (ε, M^{-1} cm^{-1})]: 462 (255), 752 (122). HR-MS (ESI, acetonitrile, positive ion) *m*/*z*: $[L^2Cu + SbF_6 + H]^+$ Calcd For $[C_{21}H_{24}CuN_4OSbF_6]^+$ (without acetonitrile) 648.02; Found 648.0219. $[L^2Cu]^+$ Calcd For $[C_{21}H_{23}CuN_4O]^+$ (without acetonitrile) 410.12; Found 410.1185. Anal. Calcd for $C_{23}H_{26}CuN_5OSbF_6$ (without acetonitrile): C 40.17, H 3.81, N 10.18. Found: C 41.73, H 4.17, N 9.98.

[L^3Cu(MeCN)][SbF_6]. In a 25 mL heart flask, HL^4 (200 mg, 0.50 mmol) and $[Cu(NCCH_3)_5][SbF_6]_2$ (370 mg, 0.50 mmol) were combined and purged with argon then dissolved in 5 mL of dry, degassed MeCN, resulting in formation of a green solution. Triethylamine (0.10 mL, 0.74 mmol) was then added, resulting in a darker green solution. At this point, the mixture was no longer air and moisture sensitive, and further workup was carried out under ambient atmosphere. The crude products were concentrated under reduced pressure to approximately 1 mL volume and selectively precipitated with 20 mL of diethyl ether. The supernatant was decanted, and the semisolid green precipitate was redissolved with 1 mL of MeCN and reprecipitated with 20 mL of diethyl ether five more times; gradual removal of colored impurities and $[HNEt_3][SbF_6]$ occurred, leaving crystalline green precipitate by the final step. The precipitate was then dissolved in 5 mL of MeCN, and an approximately equal amount of diethyl ether was gradually added until the solution became turbid yet free of green crystals. The mixture was passed through a glass fiber pad filter, removing a dark brown residue. The filtrate was concentrated under reduced pressure, dissolved fully in a minimum of MeCN (approximately 1.5 mL), layered with approximately 1.5 mL of a 1:1 MeCN/ether mixture, then approximately 20 mL of diethyl ether. After standing undisturbed for 2 days, the product was obtained as dark green crystals upon decantation of supernatant, washing with diethyl ether, and drying under vacuum. Crystals suitable for X-ray diffraction were collected from the above recrystallization prior to drying. Yield: 289 mg, 78%. Anal. Calcd for $C_{28}H_{31}CuF_6N_4OSb$: C 45.52, H 4.23, N 7.58. Found: C 45.51, H 4.13, N 7.55. UV−vis (THF, −60 °C): 700 nm (260 M^{-1} cm^{-1}).

L^1CuOAc. A solution of HL^1 (100 mg, 0.34 mmol) in anhydrous MeCN (3 mL) was added dropwise into a 20 mL scintillation vial containing $Cu(OAc)_2{\cdot}H_2O$ (74 mg, 0.37 mmol), anhydrous MeCN (3 mL), and 3 Å molecular sieves (500 mg). The reaction was stirred for 2 h at rt, resulting in a green-blue solution, which was filtered into a clean 20 mL scintillation vial using a 25 mm diameter, 0.2 mm hydrophobic PTFE syringe filter. The solvent was removed *in vacuo*. Crystalline material of the title product was obtained by vapor diffusion of anhydrous diethyl ether into a concentrated dry THF solution of **L^1CuOAc** at rt, which afforded green plate crystals that were suitable for X-ray diffraction (120 mg, 85%). UV−vis (MeCN, 25 °C) [λ_{max}, nm (ε, M^{-1} cm^{-1})]: 694 (208). Anal. Calcd for $C_{19}H_{18}CuN_4O_3$: C 55.13, H 4.38, N 13.54. Found: C 55.01, H 4.36, N 13.36.

L^2CuOAc. A solution of HL^2 (100 mg, 0.29 mmol) in anhydrous MeCN (4 mL) was added dropwise into a 20 mL scintillation vial containing $Cu(OAc)_2{\cdot}H_2O$ (62.5 mg, 0.31 mmol), anhydrous MeCN (2 mL), and 3 Å molecular sieves (1 cm). The reaction was stirred for 2 h at rt, resulting in a green-blue solution, which was filtered into a clean 20 mL scintillation vial using a 25 mm diameter, 0.2 mm hydrophobic PTFE syringe filter. The solvent was removed *in vacuo*. The green oil was allowed to stir in hexanes (5 mL) overnight, which was then decanted, and was then triturated with hexanes (2 × 5 mL). The residual solvent was removed *in vacuo* yielding a green-blue solid (103.4 mg, 77%). Crystalline material of the title product was obtained by vapor diffusion of anhydrous diethyl ether into a concentrated dry THF solution of **L^2CuOAc** at rt, which afforded blue block crystals that were suitable for X-ray diffraction. UV−vis (MeCN, 25 °C) [λ_{max}, nm (ε, M^{-1} cm^{-1})]: 694 (292). Anal. Calcd for $C_{23}H_{26}CuN_4O_3$: C 58.77, H 5.58, N 11.92. Found: C 59.77, H 5.85, N 11.76.

[(L^3Cu)$_2$OH][SbF_6]. A solution of $[L^3Cu(MeCN)][SbF_6]$ (74 mg, 0.1 mmol) in ca. 10 mL of CH_2Cl_2 was repeatedly washed with water (ca. 50 mL total volume in 5−10 mL portions) until both layers were clear and the aqueous layer had a neutral pH. Over the course of the treatment, the aqueous washes progressed from turbid pale green and acidic to colorless and neutral, while the organic layer progressed from green to turbid brown to clear cinnamon brown. The organic portion was dried with $MgSO_4$ and filtered, then selectively precipitated by addition of 10 mL of pentane with mixing. The brown precipitate was allowed to settle and the pale green supernatant was decanted, after which the former was redissolved in minimal CH_2Cl_2 (ca. 6 mL) and the above precipitation was repeated, this time resulting in a virtually colorless supernatant. The precipitate was washed with pentane and dried under vacuum overnight. Crystals suitable for diffractometry were obtained by layering a CH_2Cl_2 solution of the product with pentane and allowing to stand undisturbed for at least 24 h. Despite drying under reduced pressure, product was isolated as a solvated solid with 1 molecule of CH_2Cl_2 per [Cu]. Yield: 34 mg, 54%. UV−vis (CH_2Cl_2, 25 °C): 245 nm (>26000 M^{-1} cm^{-1}), 373 nm (8400 M^{-1} cm^{-1}), 534 nm (300 M^{-1} cm^{-1}), 747 nm (sh, 130 M^{-1} cm^{-1}). Anal. Calcd for $C_{52}H_{57}Cu_2F_6N_6O_3Sb + CH_2Cl_2$: C 50.45, H 4.71, N 6.66. Found: C 50.20, H 4.58, N 6.59.

https://doi.org/10.1021/acsomega.2c04432
ACS Omega 2022, 7, 35217−35232

$L^3Cu(OBz)$. To a solution of $[L^3Cu(MeCN)][SbF_6]$ (74 mg, 0.10 mmol) in 2 mL of CH_3CN under ambient atmosphere was added sodium benzoate (15 mg, 0.11 mmol), and the mixture was sonicated for ca. 5 min, changing color from dull green to bright sea green. After addition of 5 mL of CH_2Cl_2, undesired salts were removed by filtration through a glass fiber pad. The filtrate was evaporated under reduced pressure and redissolved in 2 mL of CH_2Cl_2, followed by selective precipitation with 5 mL of pentane, added gradually. This mixture was filtered through a glass fiber pad, yielding a bright sea green filtrate and a small amount of yellow-green precipitate. The filtrate was evaporated under reduced pressure, redissolved in 5 mL of a 1:1 CH_2Cl_2/heptane mixture, layered with 5 mL of heptane, and allowed to stand while slowly evaporating for 1 week. Bright green crystals (suitable for diffractometry) were decanted, washed with pentane, and dried under vacuum. Yield: 46 mg, 79%. UV−vis (CH_2Cl_2, 25 °C): 245 nm (>29000 M^{-1} cm^{-1}), 365 nm (8000 M^{-1} cm^{-1}), 666 nm (220 M^{-1} cm^{-1}). Anal. Calcd for $C_{33}H_{33}CuN_3O_3$: C 66.96, H 5.70, N 7.21. Found: C 66.18, H 5.56, N 6.93.

$(L^3Cu)_2CO_3$. To a 25 mL heart-shaped flask under ambient atmosphere were added HL^3 (80 mg, 0.20 mmol), anhydrous $CuCl_2$ (27 mg, 0.20 mmol), and 1.5 mL of MeOH, then mixed until fully dissolved, yielding a dull green solution. At this point, 14 mg (0.20 mmol, 2 equiv) of finely ground K_2CO_3 was added, and the mixture was sonicated for 5 min, resulting in formation of a green precipitate, which was solubilized with addition of 5 mL of CH_2Cl_2. The mixture was sonicated for an additional 15 min, during which time its color changed to a deep vibrant emerald green. Solvent was removed under low pressure, and the product residue was redissolved in CH_2Cl_2 and filtered through a pipet fitted with a glass fiber pad plug, using a total of ca. 6 mL of solvent. The solution was layered with ca. 13 mL of heptane and allowed to stand while slowly evaporating for 5 days. The resulting emerald green crystals (suitable for diffractometry) were decanted and washed with pentane, then dried under vacuum overnight. Despite this drying step, product was isolated as a solvated solid with 1 molecule of CH_2Cl_2 per [Cu]. Yield: 99.3 mg, 93%. UV−vis (CH_2Cl_2, 25 °C): 358 nm (4900 M^{-1} cm^{-1}), 679 nm (280 M^{-1} cm^{-1}). Anal. Calcd for $C_{53}H_{56}Cu_2N_6O_5$: C 60.67, H 5.47, N 7.86 Found: C 60.62, H 5.56, N 7.82.

This compound also formed spontaneously when metalations involving HL^3, Cu(II) salts, and NaOH or NaOMe were attempted under ambient atmosphere.

■ ASSOCIATED CONTENT

Supporting Information

The Supporting Information is available free of charge at https://pubs.acs.org/doi/10.1021/acsomega.2c04432.

Spectroscopic and cyclic voltammetry data (PDF)

All X-ray crystallographic data has been submitted to the CCDC. Accession numbers: L^3CuCl, 2190092; $[(L^3Cu)_2OH][SbF_6]$, 2190093; L^3CuOBz, 2190094; $[L^3CuMeCN][SbF_6]$, 2190095; $(L^3Cu)_2CO_3$, 2190096; $(L^2Cu)_2$, 2189536; L^1CuCl, 2189539; L^2CuCl, 2189535; L^1CuOAc, 2189537; L^2CuOAc, 2189538(ZIP)

■ AUTHOR INFORMATION

Corresponding Author

William B. Tolman − *Department of Chemistry, Washington University in St. Louis, St. Louis, Missouri 63130, United States;* orcid.org/0000-0002-2243-6409; Email: wbtolman@wustl.edu

Authors

Caitlin J. Bouchey − *Department of Chemistry, University of Minnesota, Minneapolis, Minnesota 55455, United States;* orcid.org/0000-0003-0729-6839

Dimitar Y. Shopov − *Department of Chemistry, Washington University in St. Louis, St. Louis, Missouri 63130, United States;* orcid.org/0000-0002-4689-4383

Aaron D. Gruen − *Department of Chemistry, University of Minnesota, Minneapolis, Minnesota 55455, United States;* orcid.org/0000-0002-5580-639X

Complete contact information is available at: https://pubs.acs.org/10.1021/acsomega.2c04432

Author Contributions

C.J.B. and D.Y.S. contributed equally.

Notes

The authors declare no competing financial interest.

■ ACKNOWLEDGMENTS

We thank the National Institutes of Health (GM47365) for financial support. X-ray diffraction data were collected using a diffractometer acquired through NSF-MRI award no. CHE-1827756. ESI-MS data were acquired on an instrument acquired via NIH grant 8P41GM103422.

■ REFERENCES

(1) Solomon, E. I.; Heppner, D. E.; Johnston, E. M.; Ginsbach, J. W.; Cirera, J.; Qayyum, M.; Kieber-Emmons, M. T.; Kjaergaard, C. H.; Hadt, R. G.; Tian, L. Copper Active Sites in Biology. *Chem. Rev.* **2014**, *114* (7), 3659−3853.

(2) Vaaje-kolstad, G.; Westereng, B.; Horn, S. J.; Liu, Z.; Zhai, H.; Sorlie, M.; Eijsink, V. G. H. An Oxidative Enzyme Boosting The. *Science* **2010**, *330*, 219−223.

(3) Walton, P. H.; Davies, G. J. On the Catalytic Mechanisms of Lytic Polysaccharide Monooxygenases. *Curr. Opin. Chem. Biol.* **2016**, *31*, 195−207.

(4) Lo Leggio, L.; Simmons, T. J.; Poulsen, J.-C. N.; Frandsen, K. E. H.; Hemsworth, G. R.; Stringer, M. A.; von Freiesleben, P.; Tovborg, M.; Johansen, K. S.; De Maria, L.; Harris, P. V.; Soong, C.-L.; Dupree, P.; Tryfona, T.; Lenfant, N.; Henrissat, B.; Davies, G. J.; Walton, P. H. Structure and Boosting Activity of a Starch-Degrading Lytic Polysaccharide Monooxygenase. *Nat. Commun.* **2015**, *6*, 5961−5969.

(5) Meier, K. K.; Jones, S. M.; Kaper, T.; Hansson, H.; Koetsier, M. J.; Karkehabadi, S.; Solomon, E. I.; Sandgren, M.; Kelemen, B. Oxygen Activation by Cu LPMOs in Recalcitrant Carbohydrate Polysaccharide Conversion to Monomer Sugars. *Chem. Rev.* **2018**, *118* (5), 2593−2635.

(6) Bertini, L.; Breglia, R.; Lambrughi, M.; Fantucci, P.; Gioia, L. De; Borsari, M.; Sola, M.; Bortolotti, C. A.; Bruschi, M. Catalytic Mechanism of Fungal Lytic Polysaccharide Monooxygenases Investigated by First-Principles Calculations. *Inorg. Chem.* **2018**, *57* (1), 86−97.

(7) Frandsen, K. E. H.; Simmons, T. J.; Dupree, P.; Poulsen, J.-C. N.; Hemsworth, G. R.; Ciano, L.; Johnston, E. M.; Tovborg, M.; Johansen, K. S.; von Freiesleben, P.; Marmuse, L.; Fort, S.; Cottaz, S.; Driguez, H.; Henrissat, B.; Lenfant, N.; Tuna, F.; Baldansuren, A.; Davies, G. J.; Lo Leggio, L.; Walton, P. H. The Molecular Basis of

Polysaccharide Cleavage by Lytic Polysaccharide Monooxygenases. *Nat. Chem. Biol.* **2016**, *12* (4), 298−303.
(8) Ciano, L.; Davies, G. J.; Tolman, W. B.; Walton, P. H. Bracing Copper for the Catalytic Oxidation of C−H Bonds. *Nat. Catal.* **2018**, *1*, 571−577.
(9) Kjaergaard, C. H.; Qayyum, M. F.; Wong, S. D.; Xu, F.; Hemsworth, G. R.; Walton, D. J.; Young, N. A.; Davies, G. J.; Walton, P. H.; Johansen, K. S.; Hodgson, K. O.; Hedman, B.; Solomon, E. I. Spectroscopic and Computational Insight into the Activation of O2 by the Mononuclear Cu Center in Polysaccharide Monooxygenases. *Proc. Natl. Acad. Sci. U. S. A.* **2014**, *111* (24), 8797−8802.
(10) Hedegård, E. D.; Ryde, U. Targeting the Reactive Intermediate in Polysaccharide Monooxygenases. *J. Biol. Inorg. Chem.* **2017**, *22* (7), 1−9.
(11) Bacik, J. P.; Mekasha, S.; Forsberg, Z.; Kovalevsky, A. Y.; Vaaje-Kolstad, G.; Eijsink, V. G. H.; Nix, J. C.; Coates, L.; Cuneo, M. J.; Unkefer, C. J.; Chen, J. C. H. Neutron and Atomic Resolution X-Ray Structures of a Lytic Polysaccharide Monooxygenase Reveal Copper-Mediated Dioxygen Binding and Evidence for N-Terminal Deprotonation. *Biochemistry* **2017**, *56* (20), 2529−2532.
(12) Caldararu, O.; Oksanen, E.; Ryde, U.; Hedegård, E. D. Mechanism of Hydrogen Peroxide Formation by Lytic Polysaccharide Monooxygenase. *Chem. Sci.* **2019**, *10* (2), 576−586.
(13) Neira, A. C.; Martínez-Alanis, P. R.; Aullón, G.; Flores-Alamo, M.; Zerón, P.; Company, A.; Chen, J.; Kasper, J. B.; Browne, W. R.; Nordlander, E.; et al. Oxidative Cleavage of Cellobiose by Lytic Polysaccharide Monooxygenase (LPMO)-Inspired Copper Complexes. *ACS Omega* **2019**, *4* (6), 10729−10740.
(14) Lindley, P. J.; Parkin, A.; Davies, G. J.; Walton, P. H. Mapping the Protonation States of the Histidine Brace in an AA10 Lytic Polysaccharide Monooxygenase Using CW-EPR Spectroscopy and DFT Calculations. *Faraday Discuss.* **2022**, *234*, 336−348.
(15) Lee, J. Y.; Karlin, K. D. Elaboration of Copper-Oxygen Mediated CH Activation Chemistry in Consideration of Future Fuel and Feedstock Generation. *Curr. Opin. Chem. Biol.* **2015**, *25*, 184−193.
(16) Kim, S.; Stahlberg, J.; Sandgren, M.; Paton, R. S.; Beckham, G. T. Quantum Mechanical Calculations Suggest That Lytic Polysaccharide Monooxygenases Use a Copper-Oxyl, Oxygen-Rebound Mechanism. *Proc. Natl. Acad. Sci. U. S. A.* **2014**, *111* (1), 149−154.
(17) Bertini, L.; Breglia, R.; Lambrughi, M.; Fantucci, P.; Gioia, L. De; Borsari, M.; Sola, M.; Bortolotti, C. A.; Bruschi, M. Catalytic Mechanism of Fungal Lytic Polysaccharide Monooxygenases Investigated by First-Principles Calculations. *Inorg. Chem.* **2018**, *57* (1), 86−97.
(18) Schröder, D.; Holthausen, M. C.; Schwarz, H. Radical-Like Activation of Alkanes by the Ligated Copper Oxide Cation (Phenanthroline)CuO+. *J. Phys. Chem. B* **2004**, *108* (38), 14407−14416.
(19) Dietl, N.; van der Linde, C.; Schlangen, M.; Beyer, M. K.; Schwarz, H. Diatomic [CuO]+ and Its Role in the Spin-Selective Hydrogen- and Oxygen-Atom Transfers in the Thermal Activation of Methane. *Angew. Chem., Int. Ed.* **2011**, *50* (21), 4966−4969.
(20) Shaffer, C. J.; Schröder, D.; Gütz, C.; Lützen, A. Intramolecular C-H Bond Activation through a Flexible Ester Linkage. *Angew. Chem., Int. Ed.* **2012**, *51* (32), 8097−8100.
(21) Elwell, C. E.; Gagnon, N. L.; Neisen, B. D.; Dhar, D.; Spaeth, A. D.; Yee, G. M.; Tolman, W. B. Copper-Oxygen Complexes Revisited: Structures, Spectroscopy, and Reactivity. *Chem. Rev.* **2017**, *117* (3), 2059−2107.
(22) Donoghue, P. J.; Tehranchi, J.; Cramer, C. J.; Sarangi, R.; Solomon, E. I.; Tolman, W. B. Rapid C-H Bond Activation by a Monocopper(III)-Hydroxide Complex. *J. Am. Chem. Soc.* **2011**, *133* (44), 17602−17605.
(23) Tehranchi, J.; Donoghue, P. J.; Cramer, C. J.; Tolman, W. B. Reactivity of (Dicarboxamide)M(II)−OH (M = Cu, Ni) Complexes − Reaction with Acetonitrile to Yield M(II)−Cyanomethides. *Eur. J. Inorg. Chem.* **2013**, No. 22−23, 4077−4084.
(24) Dhar, D.; Tolman, W. B. Hydrogen Atom Abstraction from Hydrocarbons by a Copper(III)-Hydroxide Complex. *J. Am. Chem. Soc.* **2015**, *137* (3), 1322−1329.
(25) Dhar, D.; Yee, G. M.; Spaeth, A. D.; Boyce, D. W.; Zhang, H.; Dereli, B.; Cramer, C. J.; Tolman, W. B. Perturbing the Copper(III)-Hydroxide Unit through Ligand Structural Variation. *J. Am. Chem. Soc.* **2016**, *138* (1), 356−368.
(26) Dhar, D.; Yee, G. M.; Markle, T. F.; Mayer, J. M.; Tolman, W. B. Reactivity of the Copper(III)-Hydroxide Unit with Phenols. *Chem. Sci.* **2017**, *8* (2), 1075−1085.
(27) Krishnan, V. M.; Shopov, D. Y.; Bouchey, C. J.; Bailey, W. D.; Parveen, R.; Vlaisavljevich, B.; Tolman, W. B. Structural Characterization of the [CuOR]2+Core. *J. Am. Chem. Soc.* **2021**, *143* (9), 3295−3299.
(28) Wu, T.; MacMillan, S. N.; Rajabimoghadam, K.; Siegler, M. A.; Lancaster, K. M.; Garcia-Bosch, I. Structure, Spectroscopy, and Reactivity of a Mononuclear Copper Hydroxide Complex in Three Molecular Oxidation States. *J. Am. Chem. Soc.* **2020**, *142* (28), 12265−12276.
(29) Bailey, W. D.; Dhar, D.; Cramblitt, A. C.; Tolman, W. B. Mechanistic Dichotomy in Proton-Coupled Electron-Transfer Reactions of Phenols with a Copper Superoxide Complex. *J. Am. Chem. Soc.* **2019**, *141*, 5470−5480.
(30) Itoh, S. Developing Mononuclear Copper-Active-Oxygen Complexes Relevant to Reactive Intermediates of Biological Oxidation Reactions. *Acc. Chem. Res.* **2015**, *48*, 2066−2074.
(31) Noh, H.; Cho, J. Synthesis, Characterization and Reactivity of Non-Heme 1st Row Transition Metal-Superoxo Intermediates. *Coord. Chem. Rev.* **2019**, *382*, 126−144.
(32) Mirica, L. M.; Ottenwaelder, X.; Stack, T. D. P. Structure and Spectroscopy of Copper−Dioxygen Complexes. *Chem. Rev.* **2004**, *104* (2), 1013−1046.
(33) Donoghue, P.; Gupta, A. An Anionic, Tetragonal Copper (II) Superoxide Complex. *J. Am. Chem. Soc.* **2010**, *132*, 15869−15871.
(34) Bailey, W. D.; Gagnon, N. L.; Elwell, C. E.; Cramblitt, A. C.; Bouchey, C. J.; Tolman, W. B. Revisiting the Synthesis and Nucleophilic Reactivity of an Anionic Copper Superoxide Complex. *Inorg. Chem.* **2019**, *58*, 4706−4711.
(35) Reynolds, A. M.; Lewis, E. A.; Aboelella, N. W.; Tolman, W. B. Reactivity of a 1:1 Copper−Oxygen Complex: Isolation of a Cu(II)-o-Iminosemiquinonato Species. *Chem. Commun.* **2005**, No. 15, 2014−2016.
(36) Gherman, B. F.; Tolman, W. B.; Cramer, C. J. Characterization of the Structure and Reactivity of Monocopper-Oxygen Complexes Supported by b-Diketiminate and Anilido-Imine Ligands. *J. Comput. Chem.* **2006**, *27* (16), 1950−1961.
(37) Hill, L. M. R.; Gherman, B. F.; Aboelella, N. W.; Cramer, C. J.; Tolman, W. B. Electronic Tuning of *β*-Diketiminate Ligands with Fluorinated Substituents: Effects on the O2-Reactivity of Mononuclear Cu(I) Complexes. *Dalton Trans* **2006**, *41*, 4944−4953.
(38) Reynolds, A. M.; Lewis, E. A.; Aboelella, N. W.; Tolman, W. B. Reactivity of a 1:1 Copper−Oxygen Complex: Isolation of a Cu(II)-o-Iminosemiquinonato Species. *Chem. Commun.* **2005**, No. 15, 2014−2016.
(39) Csay, T.; Kripli, B.; Giorgi, M.; Kaizer, J.; Speier, G. A Flexible Hydroxy-Bridged Dicopper Complex as Catechol Oxidase Mimic. *Inorg. Chem. Commun.* **2010**, *13* (2), 227−230.
(40) Pap, J. S.; Kripli, B.; Bányai, V.; Giorgi, M.; Korecz, L.; Gajda, T.; Árus, D.; Kaizer, J.; Speier, G. Tetra-, Penta- and Hexacoordinate Copper(II) Complexes with N3 Donor Isoindoline-Based Ligands: Characterization and SOD-like Activity. *Inorg. Chim. Acta* **2011**, *376* (1), 158−169.
(41) Taghvaee, M.; Rodríguez-Álvarez, M. J.; García-Álvarez, J.; del Río, I.; Lough, A. J.; Gossage, R. A. Amido-Pincer Complexes of Cu(II): Synthesis, Coordination Chemistry and Applications in Catalysis. *J. Organomet. Chem.* **2017**, *845*, 107−114.
(42) Anderson, O. P.; La Cour, A.; Dodd, A.; Garrett, A. D.; Wicholas, M. Syntheses and Structures of Isoindoline Complexes of

https://doi.org/10.1021/acsomega.2c04432
ACS Omega 2022, 7, 35217−35232

Zn(II) and Cu(II): An Unexpected Trinuclear Zn(II) Complex. *Inorg. Chem.* **2003**, *42* (1), 122−127.
(43) Pandiri, H.; Gonnade, R. G.; Punji, B. Synthesis of Quinolinyl-Based Pincer Copper(II) Complexes: An Efficient Catalyst System for Kumada Coupling of Alkyl Chlorides and Bromides with Alkyl Grignard Reagents. *Dalton Trans* **2018**, *47* (46), 16747−16754.
(44) Jana, O.; Mani, G. New Types of Cu and Ag Clusters Supported by the Pyrrole-Based NNN-Pincer Type Ligand. *New J. Chem.* **2017**, *41* (17), 9361−9370.
(45) Elwell, C. E.; Neisen, B. D.; Tolman, W. B. Copper Complexes of Multidentate Carboxamide Ligands. *Inorg. Chim. Acta* **2019**, *485*, 131−139.
(46) Meder, M. B.; Gade, L. H. Coordination Chemistry of 1,3-Bis(2-Pyridylimino)- and 1,3-Bis(2-Thiazolylimino)soindole Copper Complexes: Investigation of Their Catalytic Behavior in Oxidation Reactions. *Eur. J. Inorg. Chem.* **2004**, *2004* (13), 2716−2722.
(47) Bereman, R. D.; Shields, G. D.; Dorfman, J. R.; Bordner, J. Stereoelectronic Properties of Metalloenzymes. 10. a Refined Model That Mimics the Type II Copper(II) Site in Galactose Oxidase. *J. Inorg. Biochem.* **1983**, *19* (1), 75−93.
(48) Addison, A. W.; Burke, P. J.; Henrick, K. Crystal and Molecular Structure of Dipolar Spin-Coupled Dimers of an Irregularly Pentaccordinate Copper(II) Complex, [Cu(5-MeIin)(DBM)]. *Inorg. Chem.* **1982**, *21* (1), 60−63.
(49) Balogh-Hergovich, É.; Kaizer, J.; Speier, G.; Huttner, G.; Jacobi, A. Preparation and Oxygenation of (Flavonolato)Copper Isoindoline Complexes with Relevance to Quercetin Dioxygenase. *Inorg. Chem.* **2000**, *39* (19), 4224−4229.
(50) Vignesh Babu, H.; Muralidharan, K. Zn(II), Cd(II) and Cu(II) Complexes of 2,5-Bis{N-(2,6-Diisopropylphenyl)Iminomethyl}-pyrrole: Synthesis, Structures and Their High Catalytic Activity for Efficient Cyclic Carbonate Synthesis. *Dalton Trans* **2013**, *42* (4), 1238−1248.
(51) Daneshmand, P.; Fortun, S.; Schaper, F. Diiminopyrrolide Copper Complexes: Synthesis, Structures, and Rac-Lactide Polymerization Activity. *Organometallics* **2017**, *36* (19), 3860−3877.
(52) Daneshmand, P.; van der Est, A.; Schaper, F. Mechanism and Stereocontrol in Isotactic Rac-Lactide Polymerization with Copper(II) Complexes. *ACS Catal.* **2017**, *7* (9), 6289−6301.
(53) Fortun, S.; Daneshmand, P.; Schaper, F. Isotactic Rac-Lactide Polymerization with Copper Complexes: The Influence of Complex Nuclearity. *Angew. Chem., Int. Ed.* **2015**, *54* (46), 13669−13672.
(54) Sahu, R.; Padhi, S. K.; Jena, H. S.; Manivannan, V. Conversion of 2-(Aminomethyl) Substituted Pyridine and Quinoline to Their Dicarbonyldiimides Using Copper(II) Acetate. *Inorg. Chim. Acta* **2010**, *363* (7), 1448−1454.
(55) Pap, J. S.; Bányai, V.; Szilvási, D. S.; Kaizer, J.; Speier, G.; Giorgi, M. Influence of Meridional N3-Ligands on Supramolecular Assembling and Redox Behavior of Carboxylatocopper(II) Complexes. *Inorg. Chem. Commun.* **2011**, *14* (11), 1767−1772.
(56) Kaizer, J.; Pap, J.; Speier, G.; Réglier, M.; Giorgi, M. Synthesis, Properties, and Crystal Structure of a Novel 3-Hydroxy-(4H)-Benzopyran-4-One Containing Copper(II) Complex, and Its Oxygenation and Relevance to Quercetinase. *Transit. Met. Chem.* **2004**, *29* (6), 630−633.
(57) Engle, J. T.; Martić, G.; Ziegler, C. J. Investigations into the Coordination Chemistry of 1,3-Bis(2'-Benzimidazolylimino)-Isoindoline. *Macroheterocycles* **2013**, *6* (4), 353−359.
(58) Sauer, D. C.; Wadepohl, H. Variable Coordination Modes of an Active Ligand Periphery in 1,3-Bis(2-Pyridylimino)Isoindolato Copper(II) Complexes. *Polyhedron* **2014**, *81*, 180−187.
(59) Deng, Q.-H.; Wadepohl, H.; Gade, L. H. Highly Enantioselective Copper-Catalyzed Alkylation of β-Ketoesters and Subsequent Cyclization to Spirolactones/Bi-Spirolactones. *J. Am. Chem. Soc.* **2012**, *134* (6), 2946−2949.
(60) Chuang, W.-J.; Hsu, S.-P.; Chand, K.; Yu, F.-L.; Tsai, C.-L.; Tseng, Y.-H.; Lu, Y.-H.; Kuo, J.-Y.; Carey, J. R.; Chen, H.-Y.; Chen, H.-Y.; Chiang, M. Y.; Hsu, S. C. N. Reactivity Study of Unsymmetrical β-Diketiminato Copper(I) Complexes: Effect of the Chelating Ring. *Inorg. Chem.* **2017**, *56* (5), 2722−2735.
(61) Barbe, J.-M.; Habermeyer, B.; Khoury, T.; Gros, C. P.; Richard, P.; Chen, P.; Kadish, K. M. Three-Metal Coordination by Novel Bisporphyrin Architectures. *Inorg. Chem.* **2010**, *49* (19), 8929−8940.
(62) Faizi, M. S. H.; Sen, P. [Bis(Quinolin-2-Ylcarbonyl)Amido-K3N,N′,N″]Bromido(N,N-Dimethylformamide-KO)Copper(II). *Acta Crystallogr. Sect. E* **2014**, *70* (6), m206−m207.
(63) Hurley, N. J.; Hayward, J. J.; Rawson, J. M.; Murrie, M.; Pilkington, M. Exploring the Coordination Chemistry of 3,3′-Di(Picolinamoyl)-2,2′-Bipyridine: One Ligand, Multiple Nuclearities. *Inorg. Chem.* **2014**, *53* (16), 8610−8623.
(64) Kan, W.-Q.; Xia, D.-C.; Ma, J.-F. Crystal Structure of N-(5-((Pyridin-2-Yl)Methoxy)-4-Ethynyl-2,3-Dihydro-2-(Pyridin-2-Yl)-Benzofuran-3-Yl)Picolinamidecopper(I) Chloride—Methanol, Cu-(C26H16O3N5)Cl · CH3OH. *Zeitschrift für Krist. - New Cryst. Struct.* **2010**, *225* (1), 97−98.
(65) Wu, C. Y.; Su, C. C. Electronic and Bonding Properties of Mixed-Ligand Copper(II) Complexes of N-(2-Pyridylethyl)-Picolinamide (Pepa). Molecular Structures of [Cu(Pepa)(3-Methyl-Pyridine) (H2O)](ClO4), [Cu(Pepa)(4-Methylpyridine) (H2O)]-(ClO4) and [Cu(Pepa)(4-Methylimidazole) (H2O)](H2O)(ClO4). *Polyhedron* **1997**, *16* (14), 2465−2474.
(66) Brown, S. J.; Tao, X.; Stephan, D. W.; Mascharak, P. K. Synthetic Analog Approach to Metallobleomycins. 1. Syntheses, Structures and Properties of the Copper Complexes of Two Peptides Related to Bleomycins. *Inorg. Chem.* **1986**, *25* (19), 3377−3384.
(67) Brown, S. J.; Tao, X.; Wark, T. A.; Stephan, D. W.; Mascharak, P. K. Synthetic Analog Approach to Metallobleomycins. 4. New Halobridged Dimeric and Polymeric (Infinite Zigzag Chain) Complexes of Copper(II) with Peptide Ligands Related to Bleomycins. *Inorg. Chem.* **1988**, *27* (9), 1581−1587.
(68) Wang, J.; Djukic, B.; Cao, J.; Alberola, A.; Razavi, F. S.; Pilkington, M. A Novel Bis Tridentate Bipyridine Carboxamide Ligand and Its Complexation to Copper(II): Synthesis, Structure, and Magnetism. *Inorg. Chem.* **2007**, *46* (21), 8560−8568.
(69) Folgado, J. V.; Martínez-Tamayo, E.; Beltrán-Porter, A.; Beltrán-Porter, D.; Fuertes, A.; Miravitlles, C. Crystal Structure and Spectroscopic Study of [Cu(BPCA)(OH2)(O2CCH3)·H2O Complex; BPC = N-2-Pyridinylcarbonyl-2-Pyridinecarboximidate Anion. *Polyhedron* **1989**, *8* (8), 1077−1083.
(70) Lee, W. C. C.; Shen, Y.; Gutierrez, D. A.; Li, J. J. 2-Aminophenyl-1H-Pyrazole as a Removable Directing Group for Copper-Mediated C-H Amidation and Sulfonamidation. *Org. Lett.* **2016**, *18* (11), 2660−2663.
(71) Ueki, H.; Ellis, T. K.; Martin, C. H.; Soloshonok, V. A. Efficient Large-Scale Synthesis of Picolinic Acid-Derived Nickel(II) Complexes of Glycine. *Eur. J. Org. Chem.* **2003**, *2003* (10), 1954−1957.
(72) Duncan Lyngdoh, R. H.; Schaefer, H. F.; King, R. B. Metal-Metal (MM) Bond Distances and Bond Orders in Binuclear Metal Complexes of the First Row Transition Metals Titanium through Zinc. *Chem. Rev.* **2018**, *118* (24), 11626−11706.
(73) Carrier, S. M.; Ruggiero, C. E.; Houser, R. P.; Tolman, W. B. Synthesis, Structural Characterization, and Electrochemical Behavior of Copper(I) Complexes of Sterically Hindered Tris(3-Ferf-Butyl-and 3,5-Diphenylpyrazolyl)Hydroborate Ligands. *Inorg. Chem.* **1993**, *32*, 4889−4899.
(74) Mealli, C.; Arcus, C. S.; Wilkinson, J. L.; Marks, T. J.; Tbers, J. A. Structural Studies of Copper(I) Binding by Hydrotris(l-Pyrazolyl)-Borate and Hydrotris(3,5-Dimethyl-l-Pyrazolyl)Borate in the Solid State and in Solution. *J. Am. Chem. Soc.* **1976**, *98* (3), 711−718.
(75) Chang, Y. L.; Lin, Y. F.; Chuang, W. J.; Kao, C. L.; Narwane, M.; Chen, H. Y.; Chiang, M. Y.; Hsu, S. C. N. Structure and Nitrite Reduction Reactivity Study of Bio-Inspired Copper(i)-Nitro Complexes in Steric and Electronic Considerations of Tridentate Nitrogen Ligands. *Dalton Trans* **2018**, *47* (15), 5335−5341.
(76) Hsu, S. C. N.; Chang, Y.; Chuang, W.; Chen, H.; Lin, I.; Chiang, M. Y.; Kao, C.; Chen, H. Copper(I) Nitro Complex with an Anionic [HB(3,5-Me2Pz)3]- Ligand: A Synthetic Model for the

https://doi.org/10.1021/acsomega.2c04432
ACS Omega 2022, 7, 35217−35232

Copper Nitrite Reductase Active Site. *Inorg. Chem.* **2012**, *51* (17), 9297−9308.
(77) Fujisawa, K.; Tanaka, M.; Moro-oka, Y.; Kitajima, N. A Monomeric Side-On Superoxocopper(II) Complex: Cu(02)(HB(3-TBu-5-IPrpz)3). *J. Am. Chem. Soc.* **1994**, *116* (26), 12079.
(78) Chen, P.; Root, D. E.; Campochiaro, C.; Fujisawa, K.; Solomon, E. I. Spectroscopic and Electronic Structure Studies of the Diamagnetic Side-on CuII-Superoxo Complex Cu(O2)[HB(3-R-5-IPrpz)3]: Antiferromagnetic Coupling versus Covalent Delocalization. *J. Am. Chem. Soc.* **2003**, *125* (2), 466−474.
(79) Hueso-urena, F.; Esteve, V.; Debaerdemaeker, T. Copper(II) Complexes with the N,N,O-Tridentate Ligand 6-Amino-5-Formyl-Studies. *Polyhedron* **1999**, *18*, 3629−3636.
(80) Jia, W.-G.; Li, D.-D.; Dai, Y.-C.; Zhang, H.; Yan, L.-Q.; Sheng, E.-H.; Wei, Y.; Mu, X.-L.; Huang, K.-W. Synthesis and Characterization of Bisoxazolines- and Pybox-Copper(II) Complexes and Their Application in the Coupling of α-Carbonyls with Functionalized Amines. *Org. Biomol. Chem.* **2014**, *12* (29), 5509−5516.
(81) Kwiatkowski, E.; Kwiatkowski, M.; Olechnowicz, A.; Mroziński, J.; Ho, D. M.; Deutsch, E. Synthesis, Structure and Magnetic Properties of a New Chloro-Bridged Dimeric Copper Complex, Bis(μ-Chloro)Bis(8-Amino-5-Aza-4-Methyl-3-Octene-2-Onato)-Dicopper(II). *Inorg. Chim. Acta* **1989**, *158* (1), 37−42.
(82) Bu, X.-H.; Du, M.; Zhang, L.; Shang, Z.-L.; Zhang, R.-H.; Shionoya, M. Novel Copper(II) Complexes with Diazamesocyclic Ligands Functionalized by Additional Donor Group(s): Syntheses, Crystal Structures and Magnetic Properties. *J. Chem. Soc. Dalt. Trans.* **2001**, No. 5, 729−735.
(83) Bu, X. H.; Du, M.; Shang, Z. L.; Zhang, L.; Zhao, Q. H.; Zhang, R. H.; Shionoya, M. Novel Diazamesocyclic Ligands Functionalized with Pyridyl Donor Group(s) - Synthesis, Crystal Structures, and Properties of Their Copper(II) Complexes. *Eur. J. Inorg. Chem.* **2001**, *2001* (6), 1551−1558.
(84) Tuna, F.; Patron, L.; Journaux, Y.; Andruh, M.; Plass, W.; Trombe, J.-C. Synthesis and Magnetic Properties of a Series of Bi-and Tri-Nuclear Complexes of Copper(II) with the Unsymmetrical Tetradentate Schiff-Base Ligand 3-[N-2-(Pyridylethyl)Formimidoyl]-Salicylic Acid, H 2 Fsaaep, and Crystal Structures of [{Cu(Hfsaaep)-Cl} 2]. *J. Chem. Soc.* **1999**, No. 4, 539−545.
(85) Jürgens, E.; Back, O.; Mayer, J. J.; Heinze, K.; Kunz, D. Synthesis of Copper(II) and Gold(III) Bis(NHC)-Pincer Complexes. *Zeitschrift fur Naturforsch. - Sect. B J. Chem. Sci.* **2016**, *71* (10), 1011−1018.
(86) Sathyadevi, P.; Krishnamoorthy, P.; Butorac, R. R.; Cowley, A. H.; Dharmaraj, N. Novel ONN Pincer Type Copper(II) Hydrazide Complexes: An Investigation on the Effect of Electronegativity and Ring Size of Heterocyclic Hydrazides towards Nucleic Acid/Protein Binding, Free Radical Scavenging and Cytotoxicity. *Inorg. Chim. Acta* **2014**, *409*, 185−194.
(87) Boyce, D. W.; Salmon, D. J.; Tolman, W. B. Linkage Isomerism in Transition-Metal Complexes of Mixed (Arylcarboxamido)-(Arylimino)Pyridine Ligands. *Inorg. Chem.* **2014**, *53* (11), 5788−5796.
(88) Shi, Y. C.; Cheng, H. J.; Zhang, S. H. Syntheses and Crystal Structures of Copper Mixed-Ligand Complexes of Multidentate Enaminones and Acetate Anions. *Polyhedron* **2008**, *27* (16), 3331−3336.
(89) Tan, T. C.; Kracher, D.; Gandini, R.; Sygmund, C.; Kittl, R.; Haltrich, D.; Hällberg, B. M.; Ludwig, R.; Divne, C. Structural Basis for Cellobiose Dehydrogenase Action during Oxidative Cellulose Degradation. *Nat. Commun.* **2015**, *6* (1), 1−11.
(90) Chiu, E.; Hijnen, M.; Bunker, R. D.; Boudes, M.; Rajendran, C.; Aizel, K.; Oliéric, V.; Schulze-Briese, C.; Mitsuhashi, W.; Young, V.; Ward, V. K.; Bergoin, M.; Metcal, P.; Coulibaly, F. Structural Basis for the Enhancement of Virulence by Viral Spindles and Their in Vivo Crystallization. *Proc. Natl. Acad. Sci. U. S. A.* **2015**, *112* (13), 3973−3978.
(91) Labourel, A.; Frandsen, K. E. H.; Zhang, F.; Brouilly, N.; Grisel, S.; Haon, M.; Ciano, L.; Ropartz, D.; Fanuel, M.; Martin, F.; Navarro, D.; Rosso, M. N.; Tandrup, T.; Bissaro, B.; Johansen, K. S.; Zerva, A.; Walton, P. H.; Henrissat, B.; Leggio, L. Lo; Berrin, J. G. A Fungal Family of Lytic Polysaccharide Monooxygenase-like Copper Proteins. *Nat. Chem. Biol.* **2020**, *16* (3), 345−350.
(92) Haddad, M. S.; Wilson, S. R.; Hodgson, D. J.; Hendrickson, D. N. Magnetic Exchange Interactions in Binuclear Copper(II) Complexes with Only a Single Hydroxo Bridge: The x-Ray Structure of.Mu.-Hydroxo-Tetrakis(2,2'-Bipyridine)Dicopper(II) Perchlorate. *J. Am. Chem. Soc.* **1981**, *103* (2), 384−391.
(93) Harding, C. J.; McKee, V.; Nelson, J.; Lu, Q. Linear Cu−OH−Cu: Magnetic Silence for Dicopper(II) in Trigonal Bipyramidal Coordination Geometry. *J. Chem. Soc. Chem. Commun.* **1993**, *0* (23), 1768−1770.
(94) Haddad, M. S.; Hendrickson, D. N. Magnetic Properties of Binuclear Copper(II) Complexes with One Hydroxo Bridge. *Inorg. Chim. Acta* **1978**, *28* (C), L121−L122.
(95) Drew, M. G. B.; McCann, M.; Nelson, S. M. Bi-Copper(I) and Bi-Copper(II) Complexes of a 30-Membered Macrocyclic Ligand: The Inclusion of Substrate Molecules and the Crystal and Molecular Structures of a μ-Hydroxo- and a μ-Imidazolato-Complex. *J. Chem. Soc., Dalton Trans.* **1981**, No. 9, 1868−1878.
(96) Burk, P. L.; Osborn, J. A.; Youinou, M. T.; Agnus, Y.; Louis, R.; Weiss, R. Binuclear Copper Complexes: An Open and Shut Case. A Strong Antiferromagnetically Coupled.Mu.-Monohydroxo Bridged Complex. *J. Am. Chem. Soc.* **1981**, *103* (5), 1273−1274.
(97) Reger, D. L.; Pascui, A. E.; Foley, E. A.; Smith, M. D.; Jezierska, J.; Ozarowski, A. Dinuclear Metallacycles with Single M−O(H)−M Bridges [M = Fe(II), Co(II), Ni(II), Cu(II)]: Effects of Large Bridging Angles on Structure and Antiferromagnetic Superexchange Interactions. *Inorg. Chem.* **2014**, *53* (4), 1975−1988.
(98) Fry, F. H.; Spiccia, L.; Jensen, P.; Moubaraki, B.; Murray, K. S.; Tiekink, E. R. T. Binuclear Copper(II) Complexes of Xylyl-Bridged Bis(1,4,7-Triazacyclononane) Ligands. *Inorg. Chem.* **2003**, *42* (18), 5594−5603.
(99) Chiboub Fellah, F. Z.; Costes, J.-P.; Vendier, L.; Duhayon, C.; Ladeira, S.; Tuchagues, J.-P. M3- vs. μ-Hydroxido Bridges − Peripheral Function Controls the Nuclearity of Hydroxido-Bridged Copper(II) Complexes. *Eur. J. Inorg. Chem.* **2012**, *2012* (34), 5729−5740.
(100) Thompson, L. K. Structure and Magnetism in a Hydroxy Bridged Binuclear Copper(II) System with a "Tunable" Binuclear Centre. *Can. J. Chem.* **1983**, *61* (3), 579−583.
(101) Thompson, L. K.; Hartstock, F. W.; Robichaud, P.; Hanson, W. Binuclear Copper(II) Complexes of the Ligand 1,4-Di(1′-Methyl-2′-Imidazolyl)Phthalazine. Structure and Magnetism of a Hydroxyl Bridged Derivative. *Can. J. Chem.* **1984**, *62* (12), 2755−2762.
(102) Patra, A. K.; Ray, M.; Mukherjee, R. Magneto−Structural Studies of Monohydroxo-Bridged Dicopper(II) Complexes M-[Cu2L2(OH)]·2H2O (M = Na+ (1) and K+ (2); H2L = 2,6-Bis[N-(Phenyl)Carbamoyl]Pyridine). Effect of Cu-OH-Cu Bridge Angle on Antiferromagnetic Coupling. *Polyhedron* **2000**, *19* (12), 1423−1428.
(103) Folgado, J. V.; Coronado, E.; Beltrán-Porter, D.; Rojo, T.; Fuertes, A. Crystal Structure and Magnetic Properties of 1 -Aqua-μ-Hydroxo-1,2,2- Tris(Perchlorato)-1,2-Bis(2,2′;6′,2″-Terpyridine)-Dicopper(II). *J. Chem. Soc., Dalton Trans.* **1989**, No. 2, 237−241.
(104) Spodine, E.; Manzur, J.; Garland, M. T.; Kiwi, M.; Peña, O.; Grandjean, D.; Toupet, L. Magnetostructural Characterization of a Monohydroxo-Bridged, 1,1,2,2-Tetrakis(2-Pyridyl)Ethylene-Bridged Copper(II) Dimer. *J. Chem. Soc., Dalton Trans.* **1991**, No. 3, 365−369.
(105) Castro, I.; Faus, J.; Julve, M.; Lloret, F.; Verdaguer, M.; Kahn, O.; Jeannin, S.; Jeannin, Y.; Vaisserman, J. Formation in Solution, Synthesis, Crystal Structure, and Magnetic Properties of μ-Hydroxo-μ-Perchlorato-Bis[(Diethylenetriamine) Perchloratocopper(II)]. *J. Chem. Soc., Dalton Trans.* **1990**, No. 7, 2207−2212.
(106) Thompson, L. K.; Woon, T. C.; Murphy, D. B.; Gabe, E. J.; Lee, F. L.; Page, Y. Le Binuclear Copper(II) Complexes of a Series of Tetradentate Pyrazolyldiazines. Crystal and Molecular Structures of [.Mu.-3,6-Bis(3,5-Dimethyl-1-Pyrazolyl)Pyridazine-N,.Mu.-N3,.Mu.-

https://doi.org/10.1021/acsomega.2c04432
ACS Omega 2022, 7, 35217−35232

N3′,N](.Mu.-Hydroxo)Dichlorodicopper(II) Aquotrichlorocuprate Hydrate, Cu3C14H21Cl5N6O3, and [.Mu.-3,6-Bis(3,5-Dimethyl-1-Pyrazolyl)Pyridazine-N,.Mu.-N6,.Mu.-N7,N](.Mu.-Hydroxo)Tris-(Nitrato)Diaquodicopper(II) Hydrate, Cu2C14H23N9O13. *Inorg. Chem.* **1985**, *24* (26), 4719−4725.
(107) Coughlin, P. K.; Lippard, S. J. Copper(II) Chemistry in Hexaaza Binucleating Macrocycles: Hydroxide and Acetate Derivatives. *J. Am. Chem. Soc.* **1984**, *106* (8), 2328−2336.
(108) Fondo, M.; Ocampo, N.; García-Deibe, A. M.; Corbella, M.; Bermejo, M. R.; Sanmartín, J. Ferromagnetism in Dinuclear Copper(II)-Phenolate Complexes with Exogenous O-Donor Bridges: A Comparative Study. *Dalton Trans* **2005**, No. 23, 3785−3794.
(109) Koval, I. A.; Schilden, K. van der; Schuitema, A. M.; Gamez, P.; Belle, C.; Pierre, J.-L.; Lüken, M.; Krebs, B.; Roubeau, O.; Reedijk, J. Proton NMR Spectroscopy and Magnetic Properties of a Solution-Stable Dicopper(II) Complex Bearing a Single μ-Hydroxo Bridge. *Inorg. Chem.* **2005**, *44* (12), 4372−4382.
(110) Youngme, S.; Chailuecha, C.; Van Albada, G. A.; Pakawatchai, C.; Chaichit, N.; Reedijk, J. Dinuclear Triply-Bridged Copper(II) Compounds Containing Carboxylato Bridges and Di-2-Pyridylamine as a Ligand: Synthesis, Crystal Structure, Spectroscopic and Magnetic Properties. *Inorg. Chim. Acta* **2005**, *358* (4), 1068−1078.
(111) Youngme, S.; Chailuecha, C.; Van Albada, G. A.; Pakawatchai, C.; Chaichit, N.; Reedijk, J. Synthesis, Crystal Structure, Spectroscopic and Magnetic Properties of Doubly and Triply Bridged Dinuclear Copper(II) Compounds Containing Di-2-Pyridylamine as a Ligand. *Inorg. Chim. Acta* **2004**, *357* (9), 2532−2542.
(112) Geetha, K.; Nethaji, M.; Chakravarty, A. R.; Vasanthacharya, N. Y. Synthesis, X-Ray Structure, and Magnetic Properties of Ferromagnetically Coupled Binuclear Copper(II) Complexes Having a (μ-Hydroxo/Methoxo)Bis(μ-Benzoato)Dicopper(II) Core. *Inorg. Chem.* **1996**, *35* (26), 7666−7670.
(113) Sarkar, M.; Clérac, R.; Mathonière, C.; Hearns, N. G. R.; Bertolasi, V.; Ray, D. Newμ4-Oxido-Bridged Copper Benzoate Quasi-Tetrahedron and Bis-M3-Hydroxido-Bridged Copper Azide and Copper Thiocyanate Stepped Cubanes: Core Conversion, Structural Diversity, and Magnetic Properties. *Inorg. Chem.* **2010**, *49* (14), 6575−6585.
(114) Nishida, Y.; Tokii, T.; Mori, Y. A Novel U-Phenolato Binuclear Copper(II) Complex Where Two Basal Planes Are Nearly Orthogonal. *J. Chem. Soc., Chem. Commun.* **1988**, No. 10, 675−676.
(115) Sarkar, S.; Majumder, S.; Sasmal, S.; Carrella, L.; Rentschler, E.; Mohanta, S. Triple Bridged μ-Phenoxo-Bis(μ-Carboxylate) and Double Bridged μ-Phenoxo-M1,1-Azide/μ-Methoxide Dicopper(II) Complexes: Syntheses, Structures, Magnetochemistry, Spectroscopy and Catecholase Activity. *Polyhedron* **2013**, *50* (1), 270−282.
(116) Davis, A. R.; Einstein, B. Contribution from the Magnetic Exchange Interaction via a Bridging Carbonate Anion: Crystal and Molecular Structure of u-Carbonato-Bis(2,4,4,9-TetramethyI-l,5,9-Triazacyclododec-l-Ene)Dicopper(II) Perchlorate. *Inorg. Chem.* **1980**, *19* (5), 1203−1207.
(117) Company, A.; Jee, J. E.; Ribas, X.; Lopez-Valbuena, J. M.; Gómez, L.; Corbella, M.; Llobet, A.; Mahía, J.; Benet-Buchholz, J.; Costas, M.; Van Eldik, R. Structural and Kinetic Study of Reversible CO2 Fixation by Dicopper Macrocyclic Complexes. From Intramolecular Binding to Self-Assembly of Molecular Boxes. *Inorg. Chem.* **2007**, *46* (22), 9098−9110.
(118) Davis, A. R.; Einstein, F. W. B.; Curtis, N. F.; Martin, J. W. L. A Novel Mode of Carbonate Binding. Structure of Spin-Paired μ-Carbonato-Bis(2, 4, 4, 7-Tetramethyl-1, 5, 9-Triazacyclododec-l-Ene)Dicopper(II) Perchlorate. *J. Am. Chem. Soc.* **1978**, *100* (19), 6258−6260.
(119) Churchill, M. R.; Hutchinson, J. P.; Davies, G.; El-Sayed, M. A.; El-Shazly, M. F.; Rupich, M. W.; Watkins, K. O. Synthesis, Physical Properties, and Structural Characterization of μ-Carbonato-Dichlorobis(N, N, N′,N′-Tetramethyl-1, 3-Propanediamine)-Dicopper(II), LCuCl(CO3)ClCuL, a Diamagnetic Initiator for the Oxidative Coupling of Phenols by Dioxygen. *Inorg. Chem.* **1979**, *18* (8), 2296−2300.
(120) Sletten, J.; Hope, H.; Julve, M.; Kahn, O.; Verdaguer, M.; Dworkin, A. Phase Transition and Exchange Interaction in (β-Carbonato)Bis[(N,N,N′,N″,N″-Pentaethyldiethylenetriamine)-Copper(II)] Diperchlorate. *Inorg. Chem.* **1988**, *27* (3), 542−549.
(121) Kitajima, N.; Hikichi, S.; Tanaka, M.; Moro-oka, Y. Fixation of Atmospheric CO2 by a Series of Hydroxo Complexes of Divalent Metal Ions and the Implication for the Catalytic Role of Metal Ion in Carbonic Anhydrase. Synthesis, Characterization, and Molecular Structure of [LM(OH)]″ (= 1 or 2) and LM(m-C03)M. *J. Am. Chem. Soc.* **1993**, *115* (13), 5496−5508.
(122) Bernhardt, P. V. Diverse Solid-State and Solution Structures within a Series of Hexaamine Dicopper(II) Complexes. *Inorg. Chem.* **2001**, *40* (6), 1086−1092.
(123) Sorrell, T. N.; Allen, W. E.; White, P. S. Sterically Hindered [Tris(Imidazolyl)Phosphine]Copper Complexes: Formation and Reactivity of a Peroxo-Dicopper(II) Adduct and Structure of a Dinuclear Carbonate-Bridged Complex. *Inorg. Chem.* **1995**, *34*, 952−960.
(124) Kitajima, N.; Fujisawa, K.; Fujimoto, C.; Hashimoto, S.; Kitagawa, T.; Toriumi, K.; Tatsumi, K.; Nakamura, A. A New Model for Dioxygen Binding in Hemocyanin. Synthesis, Characterization, and Molecular Structure of the μ- 2:2 Peroxo Dinuclear Copper (II) Complexes, z-Pr and Ph). *J. Am. Chem. Soc.* **1992**, *114* (4), 1277−1291.
(125) Kubas, G. Tetrakis (Acetonitrile) Copper (I) Hexafluorophosphate. *Inorg. Synth.* **1979**, *19*, 90−92.
(126) Lebœuf, D.; Huang, J.; Gandon, V.; Frontier, A. J. Using Nazarov Electrocyclization to Stage Chemoselective [1,2]-Migrations: Stereoselective Synthesis of Functionalized Cyclopentenones. *Angew. Chem., Int. Ed.* **2011**, *50*, 10981−10985.
(127) Stoll, S.; Schweiger, A. EasySpin, a Comprehensive Software Package for Spectral Simulation and Analysis in EPR. *J. Magn. Reson.* **2006**, *178* (1), 42−55.
(128) Noviandri, I.; Brown, K. N.; Fleming, D. S.; Gulyas, P. T.; Lay, P. A.; Masters, A. F.; Phillips, L. The Decamethylferrocenium/Decamethylferrocene Redox Couple: A Superior Redox Standard to the Ferrocenium/Ferrocene Redox Couple for Studying Solvent Effects on the Thermodynamics of Electron Transfer. *J. Phys. Chem. B* **1999**, *103*, 6713−6722.
(129) *Bruker*, 2012; Bruker AXS, Inc.: Madison, WI.
(130) *Bruker*, 2001. Bruker AXS, Inc.: Madison, WI.
(131) Sheldrick, G. M. SHELXT − Integrated Space-Group and Crystal-Structure Determination. *Acta Crystallogr., Sect. A* **2015**, *71* (1), 3−8.
(132) Sheldrick, G. M. A. Short History of SHELX. *Acta Crystallogr., Sect. A* **2008**, *64* (1), 112−122.
(133) Dolomanov, O. V.; Bourhis, L. J.; Gildea, R. J.; Howard, J. A. K.; Puschmann, H. OLEX2: A complete structure solution, refinement and analysis program. *J. Appl. Crystallogr.* **2009**, *42*, 339−341.
(134) Hübschle, C. B.; Sheldrick, G. M.; Dittrich, B. ShelXle: A Qt Graphical User Interface for SHELXL. *J. Appl. Crystallogr.* **2011**, *44* (6), 1281−1284.

https://doi.org/10.1021/acsomega.2c04432
ACS Omega 2022, 7, 35217−35232